

AD-A269 485



2

# MICROSTRUCTURE-BASED FATIGUE LIFE PREDICTION METHODS FOR NAVAL STEEL STRUCTURES

Prepared by

R. C. McClung  
T. Y. Torng  
K. S. Chan

SECOND ANNUAL REPORT  
July 15, 1992-July 15, 1993  
SwRI Project No. 06-4414  
ONR Contract No. N00014-91-C-0214

Submitted to

Office of Naval Research  
800 N. Quincy Street  
Arlington, VA 22217-5000

July 1993

**DISTRIBUTION STATEMENT A**  
Approved for public release  
Distribution Unlimited

DTIC  
ELECTRONIC  
SEP 20 1993  
S B D



**SOUTHWEST RESEARCH INSTITUTE**  
SAN ANTONIO HOUSTON  
DETROIT WASHINGTON, DC

REPORT DOCUMENTATION PAGE

Form Approved  
OMB No. 0704-0188  
Exp. Date: Jun 30, 1986

1a. REPORT SECURITY CLASSIFICATION  
Unclassified

1b. RESTRICTIVE MARKINGS

2a. SECURITY CLASSIFICATION AUTHORITY

3. DISTRIBUTION/AVAILABILITY OF REPORT

2b. DECLASSIFICATION/DOWNGRADING SCHEDULE

Unlimited

4. PERFORMING ORGANIZATION REPORT NUMBER(S)  
06-4414/2

5. MONITORING ORGANIZATION REPORT NUMBER(S)

6a. NAME OF PERFORMING ORGANIZATION  
Southwest Research Institute

6b. OFFICE SYMBOL  
(If applicable)

7a. NAME OF MONITORING ORGANIZATION  
Office of Naval Research

6c. ADDRESS (City, State, and ZIP)  
6220 Culebra Road  
San Antonio, TX 78238-5166

7b. ADDRESS (City, State, and ZIP Code)  
800 N. Quincy Street  
Arlington, VA 22217-5000

8a. NAME OF FUNDING/SPONSORING ORGANIZATION  
Office of Naval Research

8b. OFFICE SYMBOL  
(If applicable)

9. PROCUREMENT INSTRUMENT IDENTIFICATION NUMBER  
N00014-91-C-0214

8c. ADDRESS (City, State, and ZIP)  
800 North Quincy Street  
Arlington, VA 22217-5000

10. SOURCE OF FUNDING NUMBERS

PROGRAM ELEMENT NO.	PROJECT NO.	TASK NO.	WORK UNIT ACCESSION NO.

11. TITLE (Include Security Classification)  
Microstructure-Based Fatigue Life Prediction Methods for Naval Steel Structures (Second Annual Report)

12. PERSONAL AUTHOR(S)  
R. C. McClung, T. Y. Torng, and K. S. Chan

13a. TYPE OF REPORT  
Technical

13.b TIME COVERED  
FROM 07/15/92 TO 07/15/93

14. DATE OF REPORT (Year, Month, Day)  
93/07/15

15. PAGE COUNT  
46

16. SUPPLEMENTARY NOTATION

17. COSATI CODES

FIELD	GROUP	SUB-GROUP

18. SUBJECT TERMS (Continue on reverse if necessary and identify by block number)  
Key Words: HSLA steels, fatigue life, fatigue crack growth, small cracks, modeling, microstructure, copper precipitates, probabilistic fracture mechanics

19. ABSTRACT (Continue on reverse if necessary and identify by block number)

The goal of the subject program is to develop fundamental understandings of the relationships between microstructure and fatigue damage in structural steels of interest to naval applications. Quantitative descriptions of these relationships will be incorporated within practical engineering models for the prediction of S-N fatigue life. During the second year of the program, microstructural scaling laws have been developed for fatigue crack growth (FCG) in steels. The effects of microstructure have been described by a dimensionless microstructural parameter which is defined in terms of yield stress, fatigue ductility, dislocation cell size, and dislocation barrier spacing. Fatigue crack growth data from large and small flaws have been critically compared, and the implications of this comparison for engineering fatigue life prediction are explored. Progress in the development of probabilistic fatigue life models is also summarized.

93-21687



20. DISTRIBUTION/AVAILABILITY OF ABSTRACT

UNCLASSIFIED/UNLIMITED  SAME AS RPT.  DTIC USERS

21. ABSTRACT SECURITY CLASSIFICATION  
Unclassified

22a. NAME OF RESPONSIBLE INDIVIDUAL  
R. C. McClung

22b. TELEPHONE (Include Area Code)  
(210) 522-2422

22c. OFFICE SYMBOL

## Table of Contents

LIST OF FIGURES .....	ii
ABSTRACT .....	1
INTRODUCTION .....	2
Background and Program Goals .....	2
Review of Progress During First Year .....	3
Overview of Progress During Second Year .....	3
MICROSTRUCTURAL MODELS FOR FATIGUE CRACK GROWTH .....	5
COMPARISONS OF MICROCRACKS AND LARGE CRACKS IN HSLA-80 .....	8
Large Crack Data .....	8
Microcrack Data .....	8
Comparisons .....	9
Conclusions .....	11
ENGINEERING LIFE MODELS .....	13
Smooth Specimen <i>S-N</i> Behavior .....	13
Welded Component <i>S-N</i> Behavior .....	14
PROBABILISTIC MODELING .....	16
Stochastic Fatigue Crack Growth Model .....	16
Construction of a Lognormal Random Variable Model .....	19
Construction of a Microstructure-Based SFCG Model .....	21
Overview of Probabilistic Analysis Methods .....	22
Fatigue Life Prediction Using Probabilistic Methods .....	24
Other Potential Applications of Probabilistic Modeling .....	25
FUTURE WORK .....	26
SUMMARY AND CONCLUSIONS .....	27
ACKNOWLEDGEMENTS .....	28
PUBLICATIONS AND PRESENTATIONS .....	28
REFERENCES .....	29

DTIC QUALITY INSPECTED 3

<b>Accession For</b>	
NTIS GRA&I	<input checked="" type="checkbox"/>
DTIC TAB	<input type="checkbox"/>
Unannounced	<input type="checkbox"/>
Justification .....	
By .....	
Distribution/	
Availability Codes	
Dist	Avail and/or special
A-1	

## List of Figures

Figure 1.	Comparison of experimental and calculated $da/dN$ curves for HSLA-80 steel.	31
Figure 2.	Comparison of experimental and calculated $da/dN$ curves for individual HSLA-80 steel specimens.	32
Figure 3.	Comparison of small crack data with model calculations based on the average value and standard deviations of the mean-free-path of the Cu precipitates.	33
Figure 4.	Large crack FCG data for HSLA-80 steel.	34
Figure 5.	Microcrack FCG data from square beam specimen #347.	35
Figure 6.	Microcrack FCG data from rotating beam specimens #353 and #354.	36
Figure 7.	Comparison of large crack and microcrack data based on full range $\Delta K$ .	37
Figure 8.	Comparison of large crack and microcrack data based on effective $\Delta K$ defined by the nominal ASTM approach.	38
Figure 9.	Comparison of large crack and microcrack data based on effective $\Delta K$ defined by the Newman crack closure approach.	39
Figure 10.	Comparison of large crack and microcrack data, showing linear regression of all combined data.	40
Figure 11.	Smooth specimen $S-N$ data for HSLA-80 [8].	41
Figure 12.	Welded structure $S-N$ data for HSLA-80 [9].	42
Figure 13.	Illustration of the stochastic FCG model with data from specimen #347.	43

## List of Figures (cont'd)

- |            |   |    |
|------------|---|----|
| Figure 14. | Illustration of the stochastic FCG model with data from specimens #353/354. | 44 |
| Figure 15. | Overview of planned stochastic FCG model development.                       | 45 |
| Figure 16. | Fatigue life prediction for specimens #353/354.                             | 45 |

## ABSTRACT

The goal of the subject program is to develop fundamental understandings of the relationships between microstructure and fatigue damage in structural steels of interest to naval applications. Quantitative descriptions of these relationships will be incorporated within practical engineering models for the prediction of *S-N* fatigue life. During the second year of the program, microstructural scaling laws have been developed for fatigue crack growth (FCG) in steels. The effects of microstructure have been described by a dimensionless microstructural parameter,  $\xi$ , which is defined in terms of yield stress, fatigue ductility, dislocation cell size, and dislocation barrier spacing. Fatigue crack growth data from large and small flaws have been critically compared, and the implications of this comparison for engineering fatigue life prediction are explored. Progress in the development of probabilistic fatigue life models is also summarized.

# 1. INTRODUCTION

## Background and Program Goals

The U.S. Navy currently employs HY-series steels in structural components such as submarine hulls. Since 1980, the Navy has also been evaluating the potential of HSLA (high-strength, low-alloy) steels for use in both ship and submarine construction. The introduction of these new steels has a complex impact on the design of naval structures. In some cases, design stress levels may increase to take advantage of improved properties, and this could cause significant decreases in fatigue crack initiation and propagation lives. As a result, fatigue cracking could become one of the greatest threats to structural integrity in future pressure hulls operating at higher stress levels. On the other hand, the development of new alloys with new microstructures and new welding process specifications provides the opportunity to improve the fatigue resistance of the material and, ultimately, of the structure itself.

The subject program has been motivated by the desire for improved understandings of the relationships between microstructure and fatigue damage in naval steel structures, with particular application to the prediction of fatigue life. Among the intended products of the study are improved methods for fatigue life prediction which give appropriate attention to different potential microstructures and associated microstructural influences on initiation and/or growth rates. The methods could be used to provide guidance in optimizing alloy chemistry, processing, and welding protocols for improved fatigue resistance, while also facilitating improved fitness-for-service assessments of actual or postulated cracking.

Fatigue design for naval structures is currently most often based on the stress-life (S-N) approach which relates applied stresses directly to the total life to "failure". This approach enables the analyst to take a "black box" approach to fatigue design in which relatively little must be known about the actual fatigue damage processes. But fatigue "science", such as the study of microstructural influences on fatigue damage, must look "inside" the black box to identify and characterize the physical damage processes as much as possible.

The total S-N life to "failure" is composed, in general, of three different life phases with specific physical damage processes: the nucleation of a microcrack, the growth of this microcrack until it reaches some engineering size (often on the order of millimeters), and the subsequent growth of the engineering crack to some definition of final failure. The total fatigue "life" is the sum of the lives associated with each phase. Under different conditions, one or more of the three phases may be dominant or negligibly small.

The basic technical approach of this program has been first to identify the rate-controlling fatigue mechanisms and characterize the relevant microstructures for microcrack nucleation and growth. Quantitative relationships are established between microstructural and loading parameters and fatigue damage. The second key step is then to develop practical engineering expressions to predict total S-N fatigue life which incorporate these microstructure-load-damage relationships. These life prediction models are to be expressed in an appropriate probabilistic framework which enables a quantitative assessment of the probability of S-N failure at a performance level of interest as a function of uncertainties in material/load/geometry input parameters.

## **Review of Progress During First Year**

The focus of the first year of the subject program was on experimental observations of fatigue damage in different microstructures for HSLA steels. Experimental methods were developed to study microcrack nucleation and growth with *S-N* fatigue specimens. Microstructures were modified with various heat treatments and characterized with appropriate optical and electron microscopy. Test results showed that the smooth specimen *S-N* fatigue life could be adequately characterized in terms of the nucleation and growth of individual microcracks, and that the microcrack growth phase was typically the dominant life fraction. Microcrack growth rates appeared to be only mildly dependent on microstructure, which is consistent with available data on large crack growth rates. The growth rate was found to be relatively insensitive to the ferrite matrix morphology. The potential effects of the size, volume fraction, and mean free path of the fine copper precipitates on crack growth rates were not fully resolved.

At the end of the first year, and in response to these preliminary results, we identified a set of six critical questions to guide further investigations. These questions were presented in the Annual Letter Report for FY92, along with brief descriptions of the planned technical approach to address each. These questions, in briefer form, are as follows:

1. Is there a fundamental difference between FCG rates for microcracks and large cracks in HSLA-80?
2. Does copper precipitate size and spacing have a significant effect on crack growth rates in HSLA-80?
3. Is there any significant effect of microstructure on microcrack nucleation and growth rates in HSLA steels? Why or why not?
4. What is the specific form of microcrack nucleation and growth equations which can be integrated to give good estimates of *S-N* fatigue life?
5. What is an appropriate form of a stochastic relationship to describe randomness in microcrack growth rates, and can this description provide any insight into potential microstructural effects on scatter in growth rates?
6. Is it possible to combine the stochastic description of microcrack growth rates with micro-mechanical growth rate equations and fast probability integration techniques to give an accurate description of the distribution of total *S-N* fatigue lives?

As will be noted, during the second year of the program we have substantially answered three of the six questions, while making significant progress on the remaining three.

## **Overview of Progress During Second Year**

During the second year of the program, microstructural scaling laws have been developed for FCG in steels. The effects of microstructure have been described by a dimensionless microstructural parameter,  $\xi$ , which is defined in terms of yield stress, fatigue ductility, dislocation cell

size, and dislocation barrier spacing. Fatigue crack growth data from large and small flaws have been critically compared, and the implications of this comparison for engineering fatigue life prediction are explored. Probabilistic fatigue life models are currently under development.

## 2. MICROSTRUCTURAL MODELS FOR FATIGUE CRACK GROWTH

A set of scaling laws has been developed for describing both intermittent and continuous FCG in steels in the power-law regime. The proposed scaling laws are developed on the basis that FCG occurs as the result of low-cycle fatigue failure of a crack-tip element whose width and height correspond to the dislocation cell size and barrier spacing. A detailed description of these scaling laws was presented in the manuscript, "Scaling Laws for Fatigue Crack Growth of Large Cracks in Steels," which was enclosed as an attachment to the January 30, 1993 Quarterly Report [1]. That complete discussion will not be repeated here, but it is useful to review and summarize some of the key results.

The scaling laws express the effects of microstructure in terms of a dimensionless microstructural parameter,  $\xi$ , which is defined as

$$\xi = \frac{Es}{4\sigma_y \epsilon_f' d} \quad (1)$$

where  $E$  is Young's modulus,  $\sigma_y$  is the yield strength, and  $\epsilon_f'$  is the fatigue ductility. The striation spacing,  $s$ , is taken as the dislocation cell size in the intermittent growth regime. The dislocation barrier spacing,  $d$ , is interpreted in terms of different characteristic microstructural lengths, such as the carbide spacing, grain size, lath width, or mean free path of Cu precipitates, depending on the specific microstructure under consideration.

In the intermittent growth regime, where crack growth is discontinuous, the FCG rate is given by

$$\frac{da}{dN} = \xi^{1/b} (2s)^{1-1/b} \left[ \frac{\Delta K}{E} \right]^{2b} \quad (2)$$

where  $b$  is the fatigue ductility exponent and  $\Delta K$  is the usual range of the stress intensity factor.

For continuum crack growth,  $b = 1$  and crack growth occurs at every cycle. Here Eqn. 2 is reduced to

$$\frac{da}{dN} = \xi \left[ \frac{\Delta K}{E} \right]^2 \quad (3)$$

Application of the model to a wide variety of data for HSLA and conventional ferritic, ferritic/pearlitic, and martensitic steels revealed that the lack of a strong microstructural influence on fatigue crack growth in the power-law regime is due to increasing yield strength and fatigue ductility with decreasing dislocation barrier spacing, which leads to a narrow range of  $\xi$  values (and hence a narrow range of FCG rates).

The suitability of these FCG equations for the HSLA-80 steel of particular interest in the current research program is illustrated in Figure 1. The FCG rate data shown in this figure were obtained from compact tension (large crack) tests in U.S. Navy research conducted independently at Lehigh University on the same heat of material being studied at SwRI. The slope of the lower curve, in the intermittent growth regime, is 4, while it is 2 in the high  $\Delta K$  (continuous growth) regime. Direct measurements of fatigue striation spacing found that in the intermittent regime,  $s$  was relatively constant with an average value of 0.1 to 0.2  $\mu\text{m}$ . This spacing was larger than the calculated and observed FCG rates, confirming the contention that discontinuous growth occurred in this regime. At higher  $\Delta K$  levels, the striation spacing was larger, increasing with  $\Delta K$ , and was approximately equal to the calculated and observed crack growth rates.

As indicated in the First Annual Report, the FCG data of HSLA-80 steels showed a factor of five among nominally identical, though not necessarily microstructurally identical, specimens. To investigate this difference, crack growth calculations were performed for three specimens at the upper or lower limits of the FCG rate scatter band. The calculated curves are compared with experimental FCG rate data in Figure 2. The data of Todd *et al.* [2] is also included in this figure because the data set contains  $da/dN$  results for smaller  $\Delta K$  values. Though not perfect, the good agreement between calculation and experiment nonetheless suggest that the variation in fatigue crack growth rate in HSLA-80 steels originates from variations in yield strength, fatigue ductility, and Cu-precipitate spacing, which form the dimensionless microstructural parameter,  $\xi$ . The most significant difference between specimen FZZ, which exhibited the fastest growth rate, and specimens GAH and FD1LT, which exhibited the lowest growth rates, was  $d$ , the mean free path of the Cu precipitates. Based on direct TEM measurements,  $d$  was found to be 0.46  $\mu\text{m}$  for FZZ versus 0.79  $\mu\text{m}$  for GAH and 0.89  $\mu\text{m}$  for FD1LT.

The contention that the variation in fatigue crack growth rate in HSLA-80 was due to variations in the mean-free of the Cu precipitates was tested by comparing the model calculations with small crack data. The comparison for Specimen 353, which had an equiaxed ferritic grain structure and was tested at  $R = -1$ , is shown in Figure 3. Because of  $R = -1$ ,  $\Delta K$  was computed based on the tensile load range only\*. The solid line is the crack growth rate calculated based on the mean-free path,  $d$ , of the Cu precipitates, while the dashed curves are the upper and lower bounds based on the standard deviations of the mean-free path. Figure 3 clearly shows that the statistical variations in the mean-free path of Cu precipitates accounts for the growth rate variation in small crack at high  $\Delta K$  levels, where the crack lengths were larger. In contrast, the variation in crack growth rate is substantially larger than that can be attributed to mean-free path variation at low  $\Delta K$  levels, where the crack length was extremely small ( $a$  less than about 60  $\mu\text{m}$ ). Comparison of model calculations with other small crack data for microstructures with acicular ferrite grain structures yields similar results. The conclusion drawn from these observations is that the growth of small cracks in HSLA-80 steels is controlled by the mean-free path of the Cu precipitates, and not by the morphology of the ferritic matrix. This is true for small cracks at high  $\Delta K$  levels, and might be also true at the lower  $\Delta K$  levels.

---

\* The methods of comparing large crack and small crack data on a consistent basis are discussed in the next section. The method used here is the "nominal ASTM" approach.

In commercial HSLA-80 steels, the copper content is expected to lie within 1-1.3 wt. %, which also corresponds to the range of volume fraction of Cu precipitates in percent. Since HSLA-80 steel is expected to have a minimum yield strength of 552 MPa, the average size of the Cu precipitates must be less than a certain size (usually around 5-15 nm) in order to achieve this strength level. Since both the volume fraction and the size of the precipitates are bounded within small ranges, the mean-free path of the Cu precipitates must also fall within a small range. The consequence is that the fatigue crack growth rate from HSLA-80 steels should fall within a small scatter band, as observed experimentally in large cracks. The large scatter observed in the small cracks was not due to size variation of the Cu precipitates. Additional work is needed to investigate the source of scatter in the crack growth rate variation for small cracks at low  $\Delta K$  levels.

### 3. COMPARISONS OF MICROCRACKS AND LARGE CRACKS IN HSLA-80

Experimental studies during the first year of the program focused on investigations of microcrack growth in HSLA-80 steel. These studies found that the total smooth specimen  $S-N$  fatigue life could be adequately characterized in terms of the nucleation and growth of individual microcracks. Unresolved during that first year, however, was the question of the relationship between microcrack growth and the growth of traditional "large" fatigue cracks.

A proper understanding of the relationship between microcrack and large crack growth behavior is particularly important. The microcrack growth phase is often the dominant fatigue life fraction, and so accurate modeling of this regime is often of greatest significance for accurate life predictions. On the other hand, experimental FCG rate data are most often available for large cracks (microcrack tests are much more expensive to conduct) and most theoretical models for FCG behavior are derived and validated for large crack data. The scaling laws developed under the present contract, for example, were verified through extensive comparison to large crack data. In principle, these scaling laws should also be applicable to microcracks, but this requires a certain amount of similitude between microcrack and large crack behavior. If microcrack behavior is found to be significantly different from large crack behavior in some way, then the applicability of large crack models may be called into question.

#### Large Crack Data

The available large crack data of greatest interest is presented in Figure 4. Shown here are data from four specimens tested at Lehigh University on the same heat of HSLA-80 being studied at SwRI. All tests were conducted at a stress ratio of  $R = 0.1$ . The specimen identification codes denote tests on both TL and LT orientations from both the web and flange of a structural I-beam. The data indicate that these distinctions have relatively little influence on FCG rates; differences in growth rates between the two nominally identical F-LT tests are no smaller than the differences between different configurations. These data unfortunately do not provide direct information about near-threshold behavior. In order to evaluate this regime, independent data from Todd [2] for another heat of HSLA-80 are superimposed on the figure. The Todd data clearly agree closely with the Lehigh data in the regime where the two sets overlap, but the Todd data also establish a clearly defined large crack threshold around  $\Delta K_{th} = 7 \text{ MPa}\sqrt{\text{m}}$ .

Least-squares regression of the combined data (all five data sets) between  $\Delta K = 9 \text{ MPa}\sqrt{\text{m}}$  and  $23 \text{ MPa}\sqrt{\text{m}}$  gives a Paris law slope of 3.77, only slightly lower than the theoretically estimated slope of 4.0. The scatterbands shown on Figure 4 represent  $\pm 2x$  in FCG rate and are drawn to permit easier comparisons with the microcrack data presented later.

#### Microcrack Data

Microcrack growth rate data were collected with two different specimen designs. Initial tests were conducted on beams of square cross-section 4 mm on a side by 52 mm long loaded in three-point bending. The stress ratio was maintained at nearly  $R = 0$  for the beam as a whole, but at the outer

surface of the beam, the stress ratio was different due to locally severe plasticity. To overcome this difficulty, subsequent experiments were conducted using a rotating beam specimen of hourglass shape with a minimum diameter of 4.76 mm. Here the applied stress ratio was uniformly  $R = -1$ .

Microcrack growth tests were conducted on the material in the as-received condition and in three alternative conditions created through additional heat treatments, plus one specimen fabricated from weld material. To eliminate possible sources of confusion, the initial comparisons with large crack data will incorporate only the microcrack tests in the as-received condition. This data base includes multiple cracks from one square beam specimen (347) and two rotating bending specimens (353 and 354). Specimen 347 experienced a total stress range of 840 MPa (122 ksi), Specimen 353 a total stress range of 1120 MPa (162 ksi), and Specimen 354 a total stress range of 1040 (151 ksi). From tensile tests conducted on the same heat of HSLA-80 at Lehigh University, the average yield strength is about 88 ksi (607 MPa) and the average ultimate strength about 99 ksi (683 MPa).

Crack growth rate data from these three microcrack specimens is summarized in Figure 5 (square beam specimen, 347) and Figure 6 (rotating beam specimens, 353 and 354). Individual cracks are identified here by different symbols.

### Comparisons

An initial comparison of the microcrack and large crack data based on the full-range  $\Delta K$  values, where the entire stress range  $\Delta\sigma$  is used to calculate  $\Delta K$  regardless of stress ratio, does not indicate agreement between the different data sets. See Figure 7. The slopes of the data appear to be generally similar, but differences in the intercepts leads to an apparent "layering" of the data, including disagreements between the two sets of microcrack data.

There are several differences between the various data sets which could admit some rational basis for calculating an adjusted  $\Delta K$ . The most obvious difference is that of stress ratio. The large cracks are growing at  $R = 0.1$  and the rotating bending microcracks are growing at  $R = -1$ . The square beam microcracks are growing in a local stress field with an estimated stress ratio of about  $R = -0.35$ . This local stress ratio was estimated by assuming that the maximum local stress at the outer fiber was approximately equal to the yield stress due to plastic deformation at the outer fiber, but that the stress range was still equal to the full applied (elastic) outer fiber bending stress range. A more subtle difference between the different specimens which may also have some effect is that the microcrack tests were conducted with maximum stresses near the yield stress, while the large crack tests were conducted at much lower stresses.

We have identified two alternative approaches to addressing these differences. The first approach, which we will call the "nominal ASTM approach," is based on the recommendations of ASTM Test Method E 647, "Standard Test Method for Measurement of Fatigue Crack Growth Rates." This test method instructs that  $\Delta K = K_{\max} - K_{\min}$  when  $R \geq 0$ , but that  $\Delta K$  should be calculated according to  $\Delta K = K_{\max}$  when  $R < 0$  (i.e., take only the tensile portion of the stress intensity factor range). For the particular tests under consideration here, we will write an appropriately "adjusted"  $\Delta K_{\text{eff}} = U\Delta K$ , where  $\Delta K$  is always computed as  $K_{\max} - K_{\min}$  and any stress ratio "adjustment" is expressed by the fraction  $U$ . The large crack tests have  $U = 1$ , the rotating bending tests have  $U = 0.5$ , and the square beam tests have an estimated  $U = 0.72$ .

A second approach is based on the phenomenon of plasticity-induced crack closure. Of several different proposed mechanisms for crack closure, the development of a plastic wake and the corresponding influence on residual stress fields is thought to be the most significant outside of the near-threshold regime [3]. Several different mechanics approaches have been developed to characterize plasticity-induced closure, including simple analyses based on a modified Dugdale strip-yield model, finite element analyses, superdislocation models, and boundary element models. These different formulations are nearly unanimous in their conclusions that crack opening levels outside the near-threshold regime are, in general, a function of maximum stress, stress ratio, and stress state. Many experimental observations are available to support these theoretical projections.

The specific task at hand is to estimate the magnitude of the adjustment factor  $U$ , which here functions as the effective stress intensity factor range ratio. We have chosen a specific analytical approach based on published closure models in order to eliminate the opportunity of inserting an arbitrary fudge factor. The approach is identical to a robust closure strategy under development as part of a comprehensive methodology for elastic-plastic fatigue crack growth rate prediction to be applied to aerospace propulsion systems [4]. The approach is based on the modified-Dugdale model of Newman, which has been conveniently expressed as a simple closed-form equation giving  $\sigma_{\text{open}}/\sigma_{\text{max}}$  as a function of  $\sigma_{\text{max}}/\sigma_{\text{flow}}$ ,  $R$ , and the stress state (plane stress vs. plane strain) [5]. Here  $\sigma_{\text{flow}}$  is the average of the yield and ultimate strengths. The stress state is quantified by the constraint factor  $\alpha$ , where  $\alpha = 1$  for plane stress,  $\alpha = 3$  for full plane strain, and intermediate values represent partial constraint. The Newman model is based on a center crack in an infinite plate. This model can be applied satisfactorily to other geometries by reinterpreting  $\sigma_{\text{max}}/\sigma_{\text{flow}}$  as  $K_{\text{max}}/K_{\text{flow}}$ , where  $K_{\text{flow}} = \sigma_{\text{flow}}\sqrt{\pi a}$  [6].

Based on the measured tensile properties, the estimated flow stress is 93.5 ksi (645 MPa). The stress state is identified as plane strain ( $\alpha = 3$ ) for the large crack tests on the basis of a comparison of the crack tip plastic zone sizes with characteristic specimen dimensions [7]. The estimated stress state varies for the microcrack tests, but the differences between plane stress and plane strain closure stresses under these conditions (large maximum stresses) are negligible. The maximum stress for the rotating bending specimens is just the stress amplitude  $\Delta\sigma/2$ , which is given in Table 4 of the First Annual Report. The maximum stress for the square beam specimens is estimated as  $\sigma_{\text{max}} = \sigma_{\text{ys}}$  due to the yielding at the outer fiber. The ratio of  $K_{\text{max}}/K_{\text{flow}}$  to  $\sigma_{\text{max}}/\sigma_{\text{flow}}$  for the semi-circular surface cracks which form in the microcrack tests is equal to the geometry correction factor on the stress intensity factor solution used here, 0.73. The maximum stresses (loads) for the large crack tests are small enough that no strong dependence of  $\sigma_{\text{open}}/\sigma_{\text{max}}$  on  $K_{\text{max}}/K_{\text{flow}}$  is present. On the basis of these numbers and methods, the effective stress range ratio  $U$  is calculated as  $U = 0.8$  for the large crack tests,  $U = 0.45$  for the rotating bending tests, and  $U = 0.6$  for the square beam tests.

Comparisons of the large crack and microcrack data based on these two approaches, the nominal ASTM approach and the closure approach, are presented graphically in Figures 8 and 9. Note that the two approaches give similar results. The comparison based on an explicit treatment of crack closure appears to give slightly closer agreement between large crack and microcrack data in the region where the two sets overlap, but at this point it is not our primary concern to evaluate which approach is "correct" or preferable. Instead, we only conclude from the mutual agreement that these are valid means of comparing the large crack and microcrack data, which is our primary goal here.

## Conclusions

What can be concluded from these comparisons? First of all, it appears that microcracks and large cracks grow at similar rates in the traditional large-crack power-law regime. This agreement suggests that large crack FCG relationships (including scaling laws) should also be applicable to microcracks, at least for larger microcracks.

Second, it is clear that microcracks can grow at applied stress intensity factors which are smaller than the traditional long crack threshold values,  $\Delta K_{th}$ . The microcracks exhibit no clear threshold behavior, even at smaller  $\Delta K$  values. The microcrack data do exhibit occasional crack arrests at extremely low  $\Delta K$ , but these are not consistently observed. The occasions of crack arrest which are observed may be due to unique microstructural interactions when the crack size is on the same order as the microstructure. Of greater importance to the fatigue life prediction problem, however, is the conclusion that the FCG laws used to describe microcrack growth should not, in general, include a long crack threshold. We have declined further study of large crack FCG growth very near the (large crack) threshold, since the phenomenon is not significant for fatigue life prediction based on microcrack growth relationships.

Along this line, it should be noted that we have made no special attempt here to correlate the very-near-threshold long crack data with the other data presented. It may be the case that very near the threshold, the crack closure levels increase significantly. This increase would cause a sharp decrease in the calculated driving force,  $\Delta K_{eff}$ , near threshold, which might bring the near-threshold  $da/dN$  data into line with the other data. These changes in crack closure behavior for near-threshold long cracks have been measured for other engineering materials [3]. Similar data are not currently available for HSLA-80 steels, so we are not currently able to evaluate this possibility.

A third conclusion of note is that microcracks which grow at  $\Delta K$  values below the long crack threshold appear to grow at rates which are generally consistent with a downward extrapolation of the power-law trends from the long crack regime. In other words, the long crack power-law FCG relationship may be equally applicable to shorter microcracks (in addition to longer microcracks, which were addressed above in the first conclusion). A rigorous extrapolation of the long crack power-law scatterband ( $m = 3.77$ ) passes through much of the microcrack data (see Figure 6, for example). Slightly more of the microcrack data lies above the scatterband than below it, so it is possible that the growth rates of the shortest microcracks are slightly accelerated relative to the long crack growth. Since the scatter in  $da/dN$  increases significantly for the smallest microcracks ( $a = 2$  to  $50 \mu\text{m}$ ), it is difficult to make this judgment rigorously. Further study of the problem from the statistical perspective is required.

From an engineering standpoint, it is relatively easy to address the microcrack and long crack data on an entirely consistent basis. Figure 10 shows that a single power-law fit to the combined long crack and microcrack data is very satisfactory. The slope of this particular Paris line is  $m = 3.23$ , which is only slightly smaller than the regression of the long crack data alone.

Our engineering conclusion, then, is that we can treat the microcrack data and long crack data in a similar manner for the purposes of fatigue life prediction. We also conclude that the scaling

laws derived for long crack behavior should also be applicable to the microcrack regime for HSLA-80 steels. The primary differences between the long crack and microcrack regimes involve the statistical dispersion of the data.

#### 4. ENGINEERING LIFE MODELS

Fatigue life prediction which is based on an explicit treatment of the crack growth phenomenon requires integration of the FCG equation. Consider the common choice of the simple Paris law for FCG,

$$\frac{da}{dN} = C(\Delta K)^m \quad (4)$$

where  $\Delta K$  is given by the general expression

$$\Delta K = F \Delta \sigma \sqrt{\pi a} \quad (5)$$

Note that these same expressions can be written in terms of some  $\Delta K_{\text{eff}}$  if an alternative formulation for the driving force is more appropriate. We will write everything in terms of a simple  $\Delta K$  here for convenience. If the geometry correction factor  $F$  can be treated as approximately independent of crack length, which is roughly correct for small crack problems, then the total crack propagation life,  $N_p$ , can be calculated as

$$N_p = \frac{2}{(m-2)C(F\sqrt{\pi})^m (\Delta\sigma)^m} \left\{ \frac{1}{a_i^{(m-2)/2}} - \frac{1}{a_f^{(m-2)/2}} \right\} \quad (6)$$

when  $m$  not equal to 2. Here  $a_i$  and  $a_f$  are the initial and final crack sizes. The final crack size is a function of applied stress, based on fracture mechanics arguments. This dependence, however, often has little impact on total predicted lives, since  $1/a_f^{(m-2)/2} \ll 1/a_i^{(m-2)/2}$  in many applications. If we take both of these crack sizes to be constants independent of applied stress, which is therefore an acceptable approximation from an engineering perspective, then Eqn. 6 can be simplified to the general  $S-N$  form

$$N_p = A(C, m, F) (\Delta\sigma)^{-m} \quad (7)$$

This result implies that a traditional  $S-N$  equation can be constructed directly from a FCG relationship. For our HSLA-80 steel, the implied value of  $m$  is between 3 and 4 for crack growth in the microcrack or intermittent FCG regimes. The remaining question is how accurately this derived relationship reflects actual  $S-N$  fatigue life data.

The answer to this accuracy question is dependent on the definition of " $S-N$ " data. At least two definitions are meaningful for naval structural applications. The first definition is the life of a polished smooth specimen, loaded either axially or in bending. The second definition is the life of a large-scale welded component. We will consider each definition separately.

##### Smooth Specimen $S-N$ Behavior

Available data for smooth specimen axial fatigue tests of HSLA-80 in air [8] indicate that the  $S-N$  "slope"  $m$  should be about 10-12 for tests in which the stress amplitude was less than about 100 ksi (690 MPa). See Figure 11. This slope corresponds to a fatigue strength exponent (the

exponent in the conventional stress-life expression,  $\Delta\sigma/2 = \sigma_f'(2N_f)^c$   $c = -1/m$  of about -0.08 to -0.10, which is a typical value for this class of steels. This observed value of  $m$  is significantly different from our implied value based on FCG rates. The difference is due to the influence of the crack nucleation life phase. As discussed in the introduction, the total  $S-N$  "life" can be thought of as consisting of three independent phases: nucleation, microcrack growth, and large crack growth. Under different conditions, one or more of the life phases may dominate the total life.

In particular, the nucleation phase tends to be negligibly small at relatively short lives (high stresses) and dominantly large at very long lives (low stresses). This trend is clearly evident in the microcrack growth tests reported in the First Annual Report. The average nucleation life fraction,  $N_i/N_{total}$ , was 0.233 for tests at a stress amplitude of 420 MPa, 0.113 at a stress amplitude of 520 MPa, and 0.024 at a stress amplitude of 560 MPa. The generally accepted rule of thumb is that very close to the fatigue limit, the nucleation life fraction approaches 1. This trend implies that the dependence of nucleation life on stress is extremely strong. For situations in which the nucleation phase is a significant fraction of the total life, a simple integration of the microcrack growth law will not give an entirely satisfactory description of total life. For the particular microcrack tests conducted in this program, the nucleation life fraction was typically small, and so this integration should give reasonably good life results. This method, however, will likely fail when applied to a much wider range of applied stresses.

In order to treat the total smooth specimen  $S-N$  problem more accurately, explicit attention must be given to the nucleation phase of life. The nucleation lives can be modeled by a general Coffin-Manson type of equation which relates the applied (plastic) strain range directly to  $N_i$ . We observed in the First Annual Report, based on our experimental results, that microstructure could have a pronounced effect on crack nucleation, and the nucleation equation may be able to incorporate microstructural effects explicitly. For example, if nucleation occurs at inclusions (as was the case for all fatigue tests of as-received material), then the inclusion size and the volume fraction of inclusions may be significant quantitative variables in a nucleation equation. It follows naturally that any treatment of the probabilistic  $S-N$  problem under these conditions must also address variability in the nucleation event.

It should be emphasized, however, that this quantitative treatment of the complex nucleation problem is required only when the nucleation life phase is a non-negligible fraction of the total life. When nucleation occurs relatively early in life, then a treatment based entirely on integration of the microcrack FCG equation may be satisfactory.

### **Welded Component $S-N$ Behavior**

Recent data from fatigue tests of large-scale welded structures fabricated from HSLA-80 [9] suggests an  $S-N$  slope  $m$  between 3 and 4, as shown in Figure 12. In contrast to the smooth specimen results, this slope agrees closely with the Paris exponent from the available fatigue crack growth rate data. In these structural fatigue tests, cracks initiated at relatively large defects and discontinuities in the weldments, and crack nucleation lives were relatively insignificant in comparison to total propagation lives. Simple estimates of total fatigue life based on fracture mechanics arguments (and using the same large crack baseline FCG data presented earlier in this report) were relatively successful in predicting the observed trends in experimental lives [10].

Many large-scale welded structures such as bridges and steel buildings are engineered on the basis of fatigue design curves first developed by the American Association of State Highway and Transportation Officials (AASHTO) [11]. These design curves are a set of standard  $S-N$  relationships which correspond to categories of welded details grouped according to their relative fatigue strengths. The AASHTO curves are based on the lower 95% confidence limit (using log-normal statistics) of full-scale fatigue test data. The slopes of these AASHTO design curves and similar curves published by other regulatory bodies have been fixed at  $m = 3.0$ , which is again consistent with known relationships for the fatigue crack growth behavior. It is particularly interesting that the AASHTO curves appear to provide a reasonably accurate description of the Lehigh HSLA-80 welded structure  $S-N$  data (see again Figure 12), even though the AASHTO curves were developed from tests mostly on carbon-manganese steels. This coincidence occurs because, as noted earlier in Section 2, large crack FCG rates differ relatively little among different steel microstructures.

Total life scatter in the Lehigh HSLA-80 welded structure tests was relatively large, as much as a factor of 10 for nominally identical conditions. Preliminary investigations into the origins of this scatter concluded that variations in the size of the initiating weldment defect contributed relatively little to the overall variation in life for longitudinal fillet welds. Scatter in defect size appeared to be more significant for transverse groove weld specimens. Other factors, such as variations in local weldment and crack geometry, residual stresses, material microstructure, and small flaw growth rates, will also contribute to total scatter, but these effects were not characterized in the Lehigh research.

In conclusion, acceptably accurate characterization of total life  $S-N$  behavior for welded structures based on an integration of appropriate FCG relationships appears to be feasible. Detailed attention to the crack nucleation phase of life does not appear to be necessary, although variability in the size of the initial defect (crack) may need to be addressed explicitly.

## 5. PROBABILISTIC MODELING

Fatigue crack growth is fundamentally a random phenomenon because of the macroscopic variation (from specimen to specimen) as well as the microscopic variation (along the crack path in a single specimen). This randomness may be most apparent and most significant for microcracks, when crack-microstructure interactions are also most significant. Microcrack growth rate data are often characterized by great variability, especially in comparison to growth rate data for large cracks outside of the near-threshold region. Because of this large variability, simple deterministic schemes to compute microcrack-dominated life are often not satisfactory. Algorithms based on best estimates such as mean values cannot account for the significant possibility of nonconservatively faster growth, and attempts to "envelope" the data with upper bound crack growth curves may be excessively conservative under some conditions (leading to unnecessary rejection of safe hardware).

Therefore, microcrack growth is a particularly good candidate for probabilistic methodologies. Unfortunately, microcrack growth also presents special obstacles to developing probabilistic models. In particular, it is often difficult to collect raw FCG data of sufficient quality and quantity to compute necessary probabilistic parameters. Crack length measurement is expensive and often cumbersome for microcracks, involving indirect means such as multi-step replication (rather than direct visual inspection of the specimen surface). Microcrack initiation and growth is especially unpredictable, and so it is nearly impossible to obtain data at fixed crack lengths or fixed growth intervals (as required by some probabilistic methodologies). Smooth specimens are characterized by multiple microcrack initiation and growth, so it is not usually possible to identify *a priori* a single dominant crack, and different microcracks may interact or link up later in life. These difficulties are not insurmountable, but they do influence the path to a solution.

Complete solution of the probabilistic, microstructure-based fatigue life prediction problem requires two steps. First, an appropriate stochastic FCG model, which explains reasonably the macroscopic variation (from different tests) as well as the microscopic variation (along the crack path in each test) in the material test data, must be constructed. Second, a robust, efficient, and accurate probabilistic method must be used to predict the fatigue life by using the stochastic FCG model which includes time-dependent parameters.

The development of appropriate probabilistic models is currently in progress, with most of the work to be completed during the third year of the program. The discussion that follows describes the work plan in some detail, highlighting preliminary results and deriving the key equations to be employed in subsequent research.

### Stochastic Fatigue Crack Growth Model

The selected stochastic fatigue crack growth (SFCG) model should be as simple as possible while maintaining a reasonable accuracy for the prediction of the FCG damage accumulation. The model of Ortiz [12] is an intriguing SFCG option, because it attempts to address the influence of microstructure on rate variation along the crack path. This proposed model uses a random FCG model to deal with the macroscopic variation, and an additional random noise model to deal with the microscopic variation. As a result, this model needs the probability distribution functions of the coefficients of random FCG, the probability distribution function of the variance of random noise, and the correlation length of the autocorrelation function of random noise.

Unfortunately, the Ortiz model requires that a large number of replicate test data must be available to construct accurately the required random parameters such as the joint distribution of the coefficients of random FCG, or the distribution of the variance of random noise. Under the given experimental conditions, the quantity and quality of microcrack data generated is not good enough to construct all these parameters. In addition to this data limitation, the Ortiz model also requires the crack growth measurements,  $a$  vs  $N$ , at constant growth increments,  $\Delta a$ , so that the correlation length can be measured more exactly. This requirement also violates the usual test procedure, which generates FCG data at constant  $\Delta N$  increments. Several other stochastic fatigue growth models also share the same fundamental limitation, including the Markov chain and semi-Markovian models [13, 14]. The estimation of a large Markov transition matrix usually requires a larger data base for crack size vs cycles.

*Lognormal Random Variable Model.* When only limited data are available, a lognormal random variable model proposed by Yang et. al. [15, 16] is more suitable. This model uses the simplest mathematical model for which the analytical solution is possible for many problems. Likewise, it can easily be understood by engineers. The model always results in a slightly conservative prediction. This model does not require the correlation parameter for the crack growth rate, thus eliminating the requirement for intensive test results. A few crack propagation parameters and the model statistics can be estimated from a limited amount of base-line test results, which is usually all that is available in practical applications. This model can be viewed as an ideal initial stage model for fatigue life prediction because a simple analytical function can be derived. The results calculated from this initial FCG model can be used to determine the strategies for more data acquisition or material selection. Ultimately, this model should consider other statistical uncertainties such as the microstructure parameters and the FCG model parameters in order to predict the fatigue life more accurately.

*Lognormal Random Process Model.* To account for microstructural effects, this lognormal random variable model can be coupled with a non-infinite correlation time (or correlation distance, like the Ortiz model) without necessarily having to perform computations on a large data base. In addition, the microstructural features may be modeled as random variables if enough data are available. A simple analysis procedure will be produced to estimate the correlation length by calibrating the available fatigue data with the model. The main purpose of using correlation length is to predict the fatigue life more accurately and less conservatively. This resulting stochastic model, called a lognormal random process model, is composed of a random FCG law and a stochastic process, i.e.,

$$\frac{da}{dN} = f(M, \Delta K, a, R) X_M(t) \quad (8)$$

where  $da/dN$  is the crack growth rate and  $f(\epsilon, \Delta K, a, R)$  is a user-defined function (FCG model) of microstructural features ( $M$ ), stress intensity factor range ( $\Delta K$ ), crack size ( $a$ ), and stress ratio ( $R$ ). Note that the simpler lognormal random variable model introduced earlier is actually just a special case of the more general lognormal random process model.  $X_M(t)$  represents a non-negative stationary lognormal random process which will be used to account for the combined effect of unknown contributions toward changing the crack growth rate with time,  $t$  (expressed in terms of the number of cycles,  $N$ ).  $X_M(t)$  is also considered to be a function of microstructural features. The

FCG model considered in the preliminary investigations is based on simple linear elastic fracture mechanics. When microstructural features are addressed explicitly, the scaling laws discussed in Section 2 will be employed.

Because  $X(t)$  is a nonnegative stationary lognormal random process, its logarithm, i.e.,  $\log(X(t)) = Z(t)$ , is actually a stationary gaussian (or normal) random process. This stationary gaussian random process is defined by the mean value,  $\mu_z$ , and the autocorrelation function,  $R_{ZZ}(\tau)$ . The autocorrelation function between  $Z(t)$  and  $Z(t + \tau)$  is given by

$$R_{ZZ}(\tau) = E(Z(t)Z(t + \tau)) \quad (9)$$

in which  $E(\bullet)$  is the ensemble average of the bracketed quantity. Because  $Z(t)$  is a stationary process, the autocorrelation function depends only on the time difference  $\tau$ . Because the correlation decays as the distance in space increases, it is reasonable to assume that the autocorrelation function  $R_{ZZ}(\tau)$  of the normal random process  $Z(t)$  is an exponentially decaying function of the time difference,  $\tau$ ; i.e.,

$$R_{ZZ}(\tau) = \sigma_z^2 e^{-\frac{\tau}{\xi}} \quad (10)$$

where  $\xi$  represents the correlation time and  $\xi^{-1}$  represents the measure of the correlation distance for  $Z(t)$ \*\* . As  $\xi \rightarrow \infty$ , the autocorrelation function becomes a Dirac delta function,

$$R_{ZZ}(\tau) = \sigma_z^2 \delta(\tau) \quad (11)$$

indicating that the random process  $Z(t)$  or  $X(t)$  is totally uncorrelated at any two time instants. Such a random process is referred to as the white noise process. At the other extreme as  $\xi \rightarrow 0$ , the autocorrelation function becomes a constant, i.e.,

$$R_{ZZ}(\tau) = \sigma_z^2 \quad (12)$$

indicating that the random process  $Z(t)$  or  $X(t)$  is fully correlated at any two time instants. When this condition is satisfied, the SFCG model is referred to as the lognormal random variable model. In reality, the stochastic behavior of crack propagation lies between the two extreme cases described above. To predict the fatigue life for using this stochastic fatigue model, the probabilistic analysis method must be capable of dealing with the time dependency problem effectively.

---

\*\* Note that at this point two conflicts emerge in the nomenclature due to the merger of two different scientific disciplines. In this equation,  $\sigma^2$  is the statistical variance, not the square of the stress (which is also customarily denoted by  $\sigma$ ). The second conflict is that the customary symbol for the correlation time,  $\xi$ , has been already been assigned to the dimensionless microstructural parameter in the microstructural scaling laws. In order to reduce confusion, since both variables will occasionally appear in the same equation, we will write the correlation time in this report as  $\xi_c$ .

## Construction of a Lognormal Random Variable Model

To construct the lognormal random variable model successfully, the following key factors, which can influence the accuracy of the prediction, must be addressed:

*An Appropriate Fatigue Crack Growth Model.* The choice of the crack growth law has a significant impact on crack growth predictions. A poor fit may introduce a low frequency signal into the residuals, which increases the variance and adds to the correlation of the residuals. The well-known Paris law is often adequate for the power-law FCG regime. As discussed in Ref. [6], for some materials the power-law regime may be further subdivided into intermittent and continuous growth regimes. In this case, a simple Paris law becomes inadequate and a bilinear model becomes the best choice.

*An Equal Number of Data Points for Each Test Specimen.* In the microcrack data sets generated in this study, each crack growth specimen (and often each crack) has an unequal number of data points. In particular, more crack size measurements were taken for slow growth specimens/cracks than for fast ones. This may introduce some bias to the crack growth rate calculated. As such, it clearly violates the statistical premise that each specimen is of equal weight. Consequently, the resulting statistical FCG predictions are biased toward the nonconservative side: the stochastic model tends to predict a longer propagation life or smaller crack size.

To circumvent such an error due to an unequal number of measurements for each specimen, additional data points for the primary data ( $a$  versus  $N$  or  $\log(da/dN)$  vs  $\Delta K$ ) may be added artificially to the fast crack growth specimens. The goal is to equalize the number of data points for each specimen. In most cases, the artificial points can be determined by interpolation. However, circumstances may arise where additional data points are needed outside the region of available primary data, and simple extrapolation procedures may not be satisfactory. One approach to solving this problem is first to fit the primary data for a particular specimen with the crack growth model. Then the additional data points outside the available primary data region are obtained from the model. This approach clearly does not address the point-to-point scatter as a given crack grows, but it does satisfactorily identify the central growth trends for the crack and enable acceptably accurate crack-to-crack comparisons for this preliminary SFCG model. The point-to-point scatter can be addressed by other elements of more sophisticated SFCG models.

*Data Processing Procedure.* According to the microcrack data generated in this study, each crack growth data set contains very large statistical dispersion especially in the low  $\Delta K$  regime. These statistical dispersions may be caused mainly by crack measurement error (or human error) and microstructural effects. In addition, it is very difficult to use these raw data directly in the modeling, and so data processing methods become important.

Among the available data processing methods, the secant method introduces a much larger additional statistical dispersion for the crack growth rate data than any of the incremental polynomial methods. To reduce the undesirable statistical variability of the crack growth rate data, a polynomial method should be used. While it may be desirable to use the 5-, 7-, or 9-point incremental polynomial method, the limited amount of data available may inhibit its application. Another approach is to fit all data points with the selected FCG model first. This fitted model can also be used to produce an equal number of data for each data set.

*Goodness-of-Fit Test.* Because a lognormal random variable model assumes  $X(t)$  to be a stationary lognormal random process with a median of unity, it is necessary to demonstrate that  $Z(t) = \log(X(t))$  follows the normal distribution with zero mean and standard deviation. To prove the accuracy of the model, Kolmogorov-Smirnov (K-S) tests for goodness-of-fit should be used to determine the observed K-S statistics of  $Z(t)$ . These statistics will then be used to determine if the normal distribution is acceptable or not, at a certain significance level, given the available data sets. For problems with either not enough data sets or bad quality data, the use of this lognormal random variable model must be carefully reconsidered. As suggested in Ref. [14], a bootstrap method of simulation may be used to create more available data, however, the usefulness of these data need to be evaluated.

In view of these key factors, this lognormal random variable model can be constructed as follows:

1. Take a logarithm of Eqn. (1), i.e.,

$$\log\left(\frac{da}{dN}\right) = \log(f(M, \Delta K, a, R)) + \log(X_M(t)) \quad (13)$$

2. Because the quantity and quality of microcrack data generated is limited, as discussed earlier, these data are fitted using least squares regression with the selected fatigue model to get the parameters of the model. For example, when a Paris law is used, the Paris coefficient  $C$  and Paris exponent  $m$  are determined based on the data. The process is repeated for other data sets.
3. Determine a global range of stress intensity factor and obtain an equal number of data point for each data set based on the fitted FCG models calculated in step 2.
4. Use all data created from step 3 to fit Eqn. (1) by using linear regression analysis. Since  $Z(t)$  at time  $t$  is a normal random variable,  $\log(da/dN)$  is also a normal random variable. The mean value of  $\log(da/dN) = \log(f)$ , and the standard deviation of  $\log(da/dN)$  is equal to  $\sigma_Z$ .
5. Perform K-S test for normal distribution.

#### **Example 1: 347 data (as received material)**

One example of the SFCG model in application to a particular data set is shown in Figure 13. Here the lines describing the 10%, 50% (mean value), and 90% probability of exceedance in growth rate as computed from the SFCG model are superimposed on the raw crack growth data from Specimen #347 (see First Annual Report for test details), with a simple power law as the user-selected FCG model. Final results are listed in Table 1.

As shown in Figure 13, the resulting model seems able to account approximately for all the uncertainties. However, in the higher  $\Delta K$  region (longer cracks), the estimates may be overconservative.

**Table 1. Example 1 Results Summary**

Data Set	Paris Coe. C	Paris Expo. m	Std. Dev. $\sigma_z$
347	1.08E-12	3.3792	0.422

**Example 2: 353/354 data (as received material)**

In Figure 14, the lines describing the 10%, 50% (mean value), and 90% probability of exceedance in growth rate as computed from the SFCG model are superimposed on the raw crack growth data from Specimens #353/#354 (see First Annual Report for test details), with a simple power law as the user-selected FCG model. Final results are listed in Table 2.

As discussed in Example 1, the model may be overconservative in the higher  $\Delta K$  region (larger cracks). To improve this model further, microstructural effects should be included.

**Table 2. Example 2 Results Summary**

Data Set	Paris Coe. C	Paris Expo. m	Std. Dev. $\sigma_z$
353/354	1.004E-12	2.8662	0.187

**Construction of a Microstructure-based SFCG Model**

Beginning with this simple application of a lognormal random variable model, it is planned to build a progressively more sophisticated SFCG model which explicitly addresses some of the microstructural effects. The planned steps and some of the relevant issues are briefly described below.

*Consistent Treatment of Large Crack and Microcrack Data.* Large crack and microcrack FCG data must be treated on a continuous and consistent basis not only in deterministic analysis (as discussed in Section 3) but also in probabilistic analysis. It is planned to use the same effective stress intensity factor concept proposed in Section 3 as the first step in a consistent probabilistic treatment, so that the large crack scaling laws can be applied to microcracks. Later probabilistic analysis should address and perhaps explain the increased scatter observed for the smallest microcracks.

*Microstructural Scaling Laws.* The microstructural scaling laws discussed in Section 2 will be applied as the user-defined fatigue crack growth law function,  $f$ , in Eqn. 8. In the intermittent crack growth regime, for example, this gives the general form

$$\frac{da}{dN} = \xi^{1/b} (2s)^{1-1/b} \left[ \frac{\Delta K}{E} \right]^{2b} X(t) \quad (14)$$

Microstructural variables such as the dislocation barrier spacing, the yield strength, and the fatigue ductility will be explicitly modeled as random variables in the SFCG model. Required information about the probability distribution functions for these parameters (e.g., the variation in dislocation barrier spacing) will be derived from appropriate experimental measurements. Some of this statistical information has already been presented in the First Annual Report and the January 1993 Quarterly Report.

*Treatment of the Correlation Length (Lognormal Random Process Model).* Both examples 1 and 2 showed that the simple lognormal random variable model may be too conservative. As discussed earlier, one response to this problem is to replace the simple lognormal random variable model with the lognormal random process model (including a finite correlation length). This involves a modification of the random process function  $X$  in Eqn. 8. By incorporating a correlation length into the model, the model should be able to deal with large variability observed in the small crack regime as well as long crack regime. Ortiz [12] has shown that a finite correlation length is consistent with an increase in the variability of crack growth rates at shorter crack lengths, and he postulated that this effect was attributable to microstructural effects. To determine the correlation length in practice, an efficient calibration procedure which uses the available data without performing additional experiments is required. Detailed calibration procedures will be developed later.

*General Lognormal Random Process Model with Microstructural Scaling Laws.* If the probabilistic treatment of the microstructural scaling laws and the development of a general lognormal random process model are both successful, then a final planned step is to merge these two models into a single general microstructural SFCG model.

*Overview of Planned Stochastic FCG Model Development.* An overview of the planned development of progressively more sophisticated stochastic FCG models is given in Figure 15. Beginning with the general form of the model, the first step has been to make the simplest possible choices of both the FCG function and the stochastic process. This step has been illustrated in the two examples given above. The next two steps are to independently explore more advanced choices of the FCG function and the stochastic process. The goal of these two steps is to improve the numerical quality of the probabilistic description by incorporating microstructural information. The final step is to compare and ultimately combine these two different approaches.

### **Overview of Probabilistic Analysis Methods**

As noted above in the introduction to the probabilistic modeling section, complete solution of the probabilistic, microstructure-based fatigue life prediction problem requires two steps. So far we have discussed only the first step, the development of an appropriate stochastic FCG model. The necessary second step is the development of a robust, efficient, and accurate probabilistic method to predict the fatigue life using the stochastic FCG model.

In general, the probabilistic analysis method is developed to solve a limit-state function  $g(\mathbf{X})$ . Given the joint probability density function,  $f_{\mathbf{X}}(\mathbf{x})$ , the probability of failure can be formulated as

$$\begin{aligned}
p_f &= P(g \leq 0) \\
&= \int_{\Omega} \dots \int f_{\mathbf{X}}(\mathbf{x}) d\mathbf{x}
\end{aligned}
\tag{15}$$

where  $\Omega$  is the failure region. This multiple integral is, in general, very difficult to evaluate. Alternatively, the Monte Carlo (MC) method provides a convenient, but usually time-consuming, solution. Alternative analytical procedures are available, and these are briefly discussed in the paragraphs that follow.

The first step in these analysis methods requires the transformation of a generally dependent, random vector  $\mathbf{X}$  into an independent, standardized normal vector  $\mathbf{u}$ . The Rosenblatt transformation has been suggested when the joint distribution is available [17, 18]. If only the marginal distributions and the covariances are known, a transformation can be made to generate a joint normal distribution that satisfies the given correlation structure.

By transforming  $g(\mathbf{X})$  to  $g(\mathbf{u})$ , the most probable point (MPP) in the  $u$ -space,  $\mathbf{u}^*$ , is located. The MPP  $\mathbf{u}^*$  is the point that defines the minimum distance,  $\beta$ , from the origin ( $\mathbf{u} = 0$  point) to the limit-state surface. This point is most probable because it has the maximum joint probability density on the limit-state surface. The MPP may be found by using optimization, advanced mean value (AMV), or other iteration schemes.

Next, the  $g(\mathbf{u})$  or  $g(\mathbf{X})$  function is approximated by a polynomial that approximates the true function in the vicinity of the MPP. Once the approximate function is obtained, the associated failure probability can be computed. If the  $g(\mathbf{u})$  formulation is used, several analytical solutions are available for linear and quadratic functions [19, 20]. For example, the first-order reliability method (FORM) estimate is:

$$P(g \leq 0) \approx \Phi(-\beta) \tag{16}$$

and the asymptotic second-order reliability method (SORM) estimate, derived by Breitung [20], is:

$$P(g \leq 0) \approx \Phi(-\beta) \prod_{j=1}^{n-1} (1 + \beta \kappa_j)^{-1/2}, \quad \beta \rightarrow \infty \tag{17}$$

where  $\Phi(\cdot)$  is the cdf of a standard normal distribution and  $\kappa_j, j = 1, \dots, n - 1$  are the main curvatures of the limit-state surface at  $\mathbf{u}^*$ .

However, for complex problems that require computation-intensive computer programs, it is very important to use an efficient method to calculate the cumulative distribution function of the response. The AMV and AMV+ methods were developed to search for the MPP with fewest extra  $g$ -function calculations by comparing with the conventional mean-based second-moment method (MVFOSM). AMV and AMV+ methodologies are discussed in greater detail in Ref. [21].

## Fatigue Life Prediction Using Probabilistic Methods

The choice of a specific probabilistic method depends on the complexity of the particular stochastic fatigue crack growth model under consideration. In the following, the probabilistic methods anticipated to be selected to different SFCG models are briefly discussed.

*Lognormal Random Variable Model.* By using a lognormal random variable model, an analytical function for the probability distribution for crack length at the given time (or, alternatively, the probability distribution for time at the given crack length) can be derived and used to predict the fatigue life. Because only one lognormal random variable is considered, this problem can be solved by most of the probabilistic approaches. Total required calculation effort is minimum. In addition, this model can easily be extended to include inspection and repair strategy.

*Lognormal Random Variable Model With Microstructural Scaling Laws.* This model can be solved using the same analysis strategy as the previous lognormal random variable model, but more random variables are considered in the model. Therefore, more advanced probabilistic methods may be needed to solve the problem.

*Lognormal Random Process Model.* By using a lognormal random process model, crack growth at any length becomes correlated. In this case, no explicit function can be derived. To predict the fatigue life, two approaches will be considered. First, a Monte Carlo approach proposed in Ref. [15] will be used, and second, an analytical approach will be used, as described below.

The MC approach is a simple but time-consuming method, especially for far-tail probability regions, because MC is a simulation process which requires many simulations. Each simulation includes at least three steps: first, generate a random process for the stationary gaussian process; second, integrate this random process with the FCG model; and third, calculate the crack length as a function of time. The process is repeated when the required sample number is reached. All crack size functions are stored and used to construct the crack length distribution function.

The analytical approach is based on a Markov process model proposed by Lin and Yang [22]. This model is fracture mechanics-based, whereas the Bogdanoff-Kozin model [13] is not. The following autocorrelation function is used:

$$\begin{aligned} R_{zz}(\tau) &= 2\beta(1 - |\tau|/\Delta) & |\tau| \leq \Delta \\ &= 0 & \text{otherwise} \end{aligned} \tag{18}$$

With this assumption, a complicated analytical function for crack size probability distribution function at the given time can then be derived. However, this analytical function is based on an assumed autocorrelation function. To fully utilize this analytical function, an approximate function to simulate the difference between Eqn. 10 and Eqn. 18 will be included in the previous analytical function. By using this updated function, an AMV+ based probabilistic method will be used to compute the final probabilistic results.

*Lognormal Random Process Model Plus Microstructural Scaling Laws.* This model can be solved using the same analysis strategy as the previous lognormal random process model, but more random variables are considered in the model.

It should be noted that for all of these SFCG laws, appropriate attention must also be given to the determination of the initial crack size and final critical crack size conditions in order to perform a complete life prediction. If the nucleation phase is a significant fraction of the total life (e.g., smooth specimen life predictions), then the nucleation life must also be modeled. These factors may introduce additional sources of uncertainty, and further influence the selection of the probabilistic method.

### **Example 3: 353/354 fatigue life prediction using lognormal random variable model**

The initial crack size and the crack initiation life selected for this data set are  $9.43 \mu\text{m}$  and  $10^4$  cycles, respectively. By using both data and the results shown in Table 2, the crack growth curves at 10%, 50% (mean value), and 90% can be easily calculated, as shown in Figure 16. As predicted, the 90% and 10% curves have incorporated the data well except in the small crack regime. The disagreement in this regime is due, at least in part, to the specific selections of initial crack size and initiation life in this example. Therefore, it is important that both values be selected carefully.

### **Other Potential Applications of Probabilistic Modeling**

Development of the probabilistic models discussed above provides the opportunity and the technical foundation to solve additional aspects of the fatigue life problem. Substantial progress on some of these auxiliary issues is not anticipated under the current contract effort, but the potential extensions are worthy of brief note.

*Design Strategy: Probabilistic Sensitivity Factors.* Probabilistic sensitivity factors are a significant by-product of the probabilistic analysis. These factors provide guidance on the manner in which input uncertainties influence variability in the response function, identify those random variables which are most significant for this variability, and help to determine the optimum strategy for subsequent design analysis. Probabilistic sensitivity factors will be of particular benefit in the current contract effort to help identify those microstructural variables which are of greatest significance for both the mean value and the variability of the fatigue life, and to assess the relative significance of microstructural effects for the total fatigue life problem. They have the potential to play a stronger role in future efforts to design better critical experiments and, ultimately, to influence the direction of future engineering design strategies for naval structures.

*Life Extension (Remaining Life) Prediction.* Inspection and repair strategies are useful for extending the total fatigue life. However, calculation of the remaining life after an inspection and repair process introduces new challenges. To implement the analysis, the following quantities must be determined or developed: an initial quality of the damaged element before and after repair; a stochastic FCG model; a probability of detection curve, which is used to simulate a specific inspection technique; and advanced probabilistic methods for determining the probability of detection or remaining life. These expanded models can be used to determine both an inspection strategy (when to inspect) and a repair strategy (whether to replace or repair).

## 6. FUTURE WORK

Research in the third year of the subject contract will emphasize further development of the stochastic fatigue crack growth models, as outlined in Section 5. Microstructural effects will be incorporated into the SFCG models in two different ways. First, the deterministic microstructural scaling laws presented in Section 2 will be employed as the user-defined FCG law in the SFCG model. Appropriate microstructural parameters, such as the dislocation barrier spacing and yield strength, will be defined as random variables with specified mean values and standard deviations. Second, a lognormal random process model with a finite correlation length will be explored as a means of describing the increased dispersion observed at smaller crack lengths. A suitable probabilistic analysis method will be chosen to solve the resulting SFCG model and perform actual fatigue life prediction calculations.

Development of engineering life models will be integrated closely with this stochastic model development task. The engineering life model task will insure that the engineering problem being addressed by the SFCG model is properly defined and that the results are relevant and meaningful to practical engineering challenges. The final engineering life model is expected to be largely inseparable from the final stochastic FCG model.

For the past two years, research in the task on modeling of microstructure/fatigue relationships has been focused on the crack growth problem. The result of this effort was the development of scaling laws for fatigue crack growth in steels. In the coming year, a smaller additional research effort will focus on developing scaling laws for nucleation of microcracks. The nucleation phase was shown in Section 4 to be significant for total  $S-N$  life under some conditions (e.g., smooth specimens at long lives), although under other conditions the nucleation phase is negligible. The role of microstructural parameters such as dislocation cell size, dislocation barrier spacing, and inclusion size on microcrack nucleation life will be established. The effects of microstructure on fatigue life will be elucidated by examining individually as well as totally its influence on nucleation and propagation lives. These fatigue life relations will be further verified for HSLA-80 and HY-80 steels.

## 7. SUMMARY AND CONCLUSIONS

1. Scaling laws have been developed to explain/predict the effects (or lack of effects) of microstructure on fatigue crack growth rates in steels.
2. The critical microstructural feature of HSLA-80 steel for fatigue crack growth rates appears to be the Cu precipitates.
3. Properly correlated microcrack behavior (e.g., average FCG rates) in HSLA-80 steel appears to be consistent with large crack behavior.
4. Fatigue crack growth equations appear to be adequate to describe total  $S-N$  fatigue lives in HSLA-80 steel when nucleation lives are negligibly short (e.g., welded structures).
5. A lognormal random process stochastic FCG model appears to be a suitable choice to address the dispersion in microcrack growth rate data.

## ACKNOWLEDGMENTS

The support of ONR Scientific Officer Dr. A. K. Vasudevan is gratefully acknowledged. Appreciation is extended to Dr. D. L. Davidson for helpful discussions. The authors are pleased to recognize the technical assistance of Dr. Y.-M. Pan with TEM, Mr. J. Campbell with SEM, and Mr. T. S. Grant with data analysis. Dr. R. J. Dexter, ATLSS Center, Lehigh University, is thanked for supplying HSLA-80 data and tested specimens. Additional thanks are extended to Dr. J. A. Todd and Mr. L. Chen of the Illinois Institute of Technology for supplying their HSLA crack growth data.

## PUBLICATIONS AND PRESENTATIONS

"Scaling Laws for Fatigue Crack Growth of Large Cracks in Steels," by K. S. Chan, has been accepted for publication in *Metallurgical Transactions A*, and is currently in press.

"Scaling Laws for Fatigue Crack Growth of Large Cracks in Steels," by K. S. Chan, has been submitted for presentation at the 1994 TMS Annual Meeting, San Francisco, CA, February 27 - March 3, 1994.

"Microstructure-Based Fatigue Life Prediction Using Probabilistic Analysis Methods," by T. Y. Torng and R. C. McClung, has been submitted in abstract form for presentation at the 35th AIAA/ASME/ASCE/AHS/ASC Structures, Structural Dynamics, and Materials Conference, April 1994.

## REFERENCES

1. K. Chan, R. C. McClung, and T. Y. Torng, "Microstructure-Based Fatigue Life Prediction Methods for Naval Steel Structures," Quarterly Report, ONR Contract N00014-91-C-0214, January 30, 1993.
2. J. A. Todd, L. Chen, E. Y. Yankov, and H. Tao, "A Comparison of the Near-Threshold Corrosion Fatigue Crack Propagation Rates in Mil S-24645 HSLA Steel and Its Weld Metal," *ASME Journal of Offshore Mechanics and Arctic Engineering*, Vol. 115, 1993, pp. 131-136.
3. R. C. McClung, "The Influence of Applied Stress, Crack Length, and Stress Intensity Factor on Crack Closure," *Metallurgical Transactions A*, Vol. 22A, 1991, pp. 1559-1571.
4. "Elastic-Plastic and Fully Plastic Fatigue Crack Growth," NASA Contract NAS8-37828, Southwest Research Institute Project No. 06-5013, 1992-1994.
5. J. C. Newman, Jr., "A Crack Opening Stress Equation for Fatigue Crack Growth," *International Journal of Fracture*, Vol. 24, 1984, pp. R131-R135.
6. R. C. McClung, "Finite Element Analysis of Specimen Geometry Effects on Fatigue Crack Closure," Topical Report to NASA George C. Marshall Space Flight Center, NASA Contract NAS8-37828, April 1993.
7. R. C. McClung, "Closure and Growth of Mode I Cracks in Biaxial Fatigue," *Fatigue and Fracture of Engineering Materials and Structures*, Vol. 12, 1989, pp. 447-460.
8. T. W. Montemarano, B. P. Sack, J. P. Gudas, M. G. Vassilaros, and H. H. Vanderveldt, "High Strength Low Alloy Steels in Naval Construction," *Journal of Ship Production*, Vol. 2, 1986, pp. 145-162.
9. R. J. Dexter, J. W. Fisher, and J. E. Beach, "Fatigue Behavior of Welded HSLA-80 Members," ASME Offshore Mechanics and Arctic Engineering Conference, Glasgow, UK, June 1993.
10. G. R. Kober, R. J. Dexter, E. J. Kaufmann, B. T. Yen, and J. W. Fisher, "The Effect of Welding Discontinuities on the Variability of Fatigue Life," *Fracture Mechanics: 25th Volume, ASTM STP 1220*, in press.
11. *Standard Specification for Highway Bridges*, 14th ed., The American Association of State Highway Transportation Officials, Washington, DC, 1989.
12. K. Ortiz and A. Kiremidjian, "Stochastic Modeling of Fatigue Crack Growth," *Engineering Fracture Mechanics*, Vol. 29, 1988, pp. 317-334.
13. F. Kozin and J. L. Bogdanoff, "A Critical Analysis of Some Probabilistic Models of Fatigue Crack Growth," *Engineering Fracture Mechanics*, Vol. 14, 1981, pp. 59-89.
14. F. H. Al-Sugair and A. S. Kiremidjian, "A Semi-Markovian Model For Low-Cycle Elastic-Plastic Fatigue Crack Growth," *Engineering Fracture Mechanics*, Vol. 34, 1989, pp. 1197-1207.

15. J. N. Yang, W. H. Hsi, and S. D. Manning, *Stochastic Crack Propagation With Applications To Durability and Damage Tolerance Analyses*, AFWAL-TR-85-3062, 1985.
16. G. C. Salivar, J. N. Yang, and B. J. Schwartz, "A Statistical Model For The Prediction of Fatigue Crack Growth Under A Block Type Spectrum Loading," *Engineering Fracture Mechanics*, Vol. 31, 1988, pp. 371-380.
17. A. H.-S. Ang, and W. H. Tang, *Probability Concept in Engineering Planning and Design, Volume II: Decision, Risk, and Reliability*, New York, John Wiley & Sons, Inc., 1984.
18. H. O. Madsen, S. Krenk, and N. C. Lind, *Methods of Structural Safety*, Englewood Cliffs, New Jersey, Prentice Hall, Inc., 1986.
19. L. Tvedt, "Distribution of Quadratic Forms in Normal Space — Application to Structural Reliability," *Journal of Engineering Mechanics*, ASCE, Vol. 116, 1990, pp. 1183-1197.
20. K. Breitung, "Asymptotic Approximations for Probability Integrals," *Probabilistic Engineering Mechanics*, Vol. 4, 1989.
21. Y.-T. Wu, O. H. Burnside, and T. A. Cruse, "Probabilistic Methods for Structural Response Analysis," *Computational Probabilistic Methods*, ASME, Vol. 93, 1988; also published in *Computational Mechanics of Reliability Analysis*, W.K. Liu and T. Belytschko (eds.), Elsevier International, Ch. 7, 1989, pp. 181-196.
22. Y. K. Lin and J. N. Yang, "A Stochastic Theory of Fatigue Crack Propagation," *AIAA Journal*, Vol. 23, 1985, pp. 117-124.

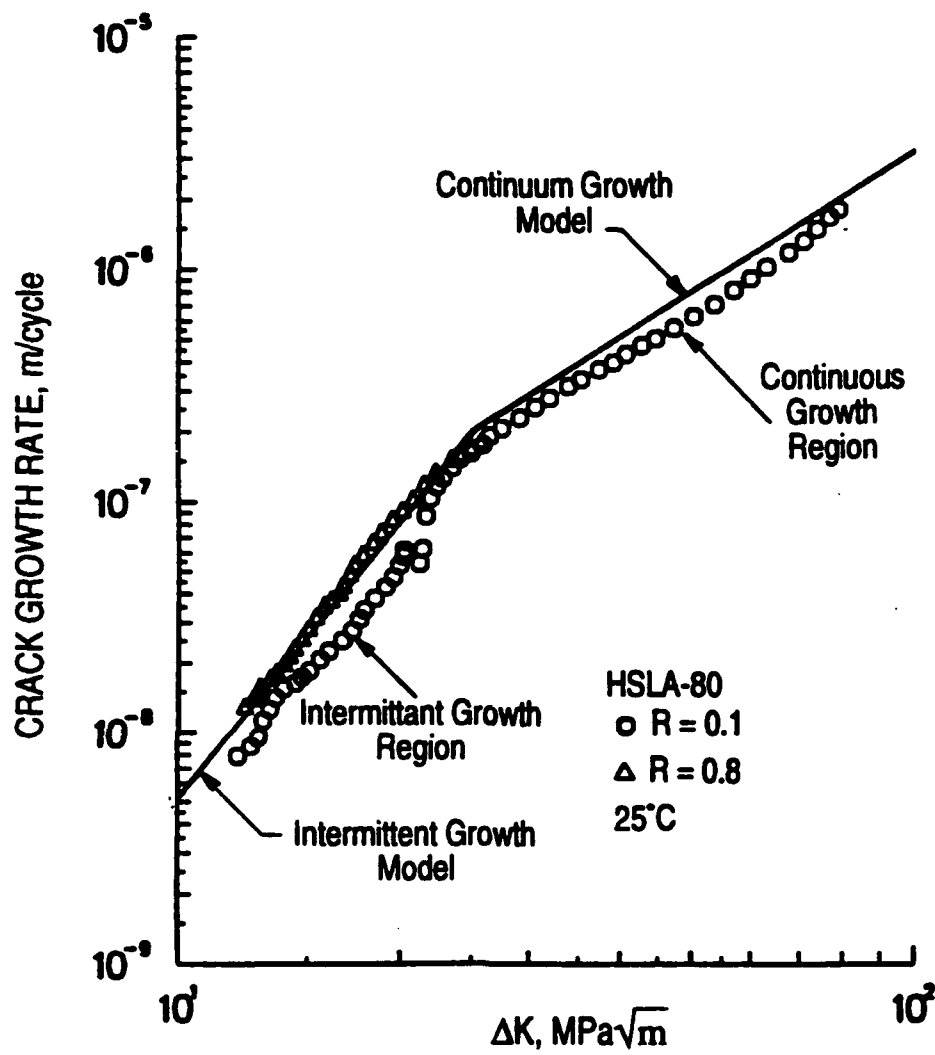


Figure 1. Comparison of experimental and calculated  $da/dN$  curves for HSLA-80 steel.

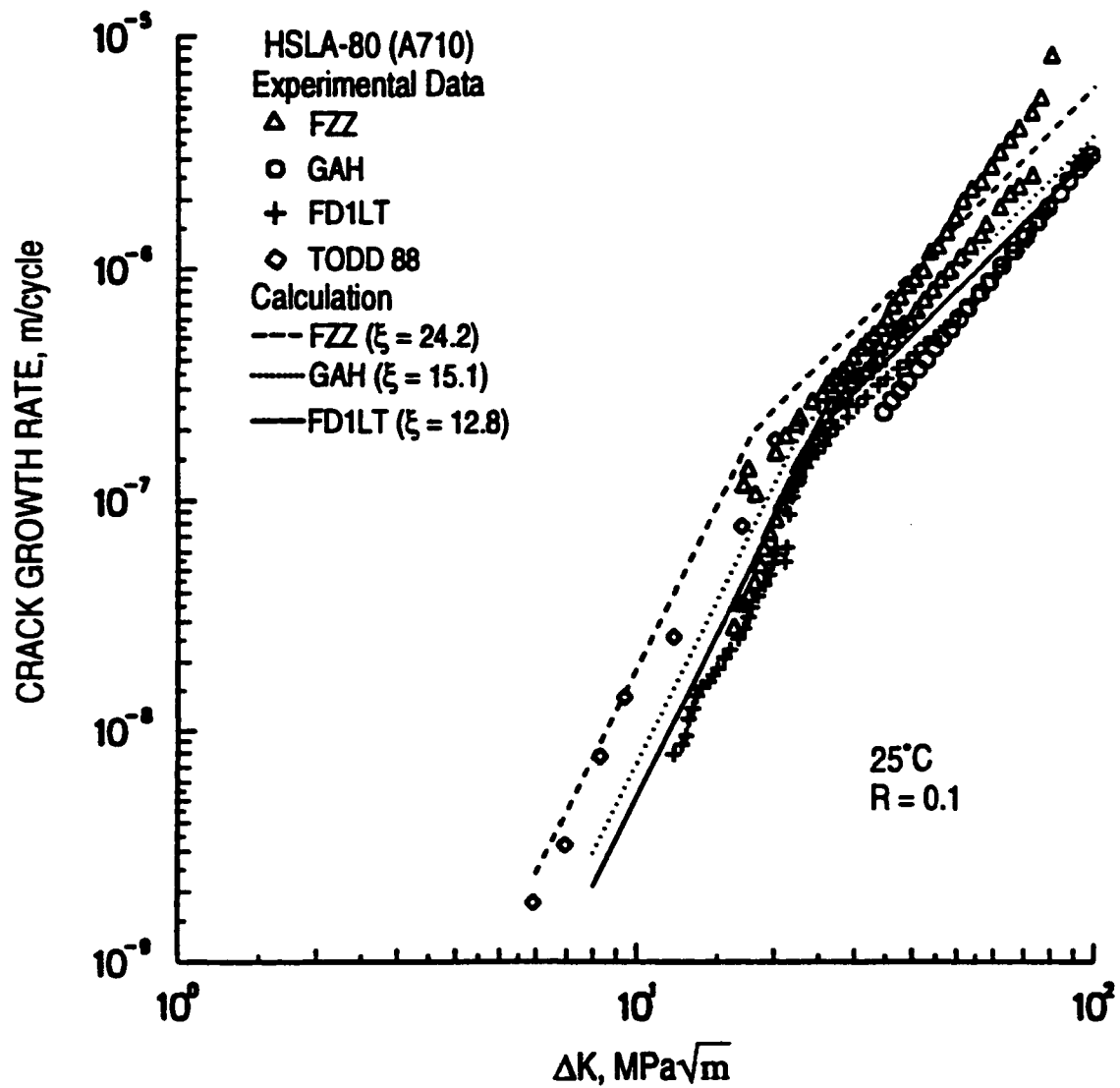


Figure 2. Comparison of experimental and calculated  $da/dN$  curves for individual HSLA-80 steel specimens.

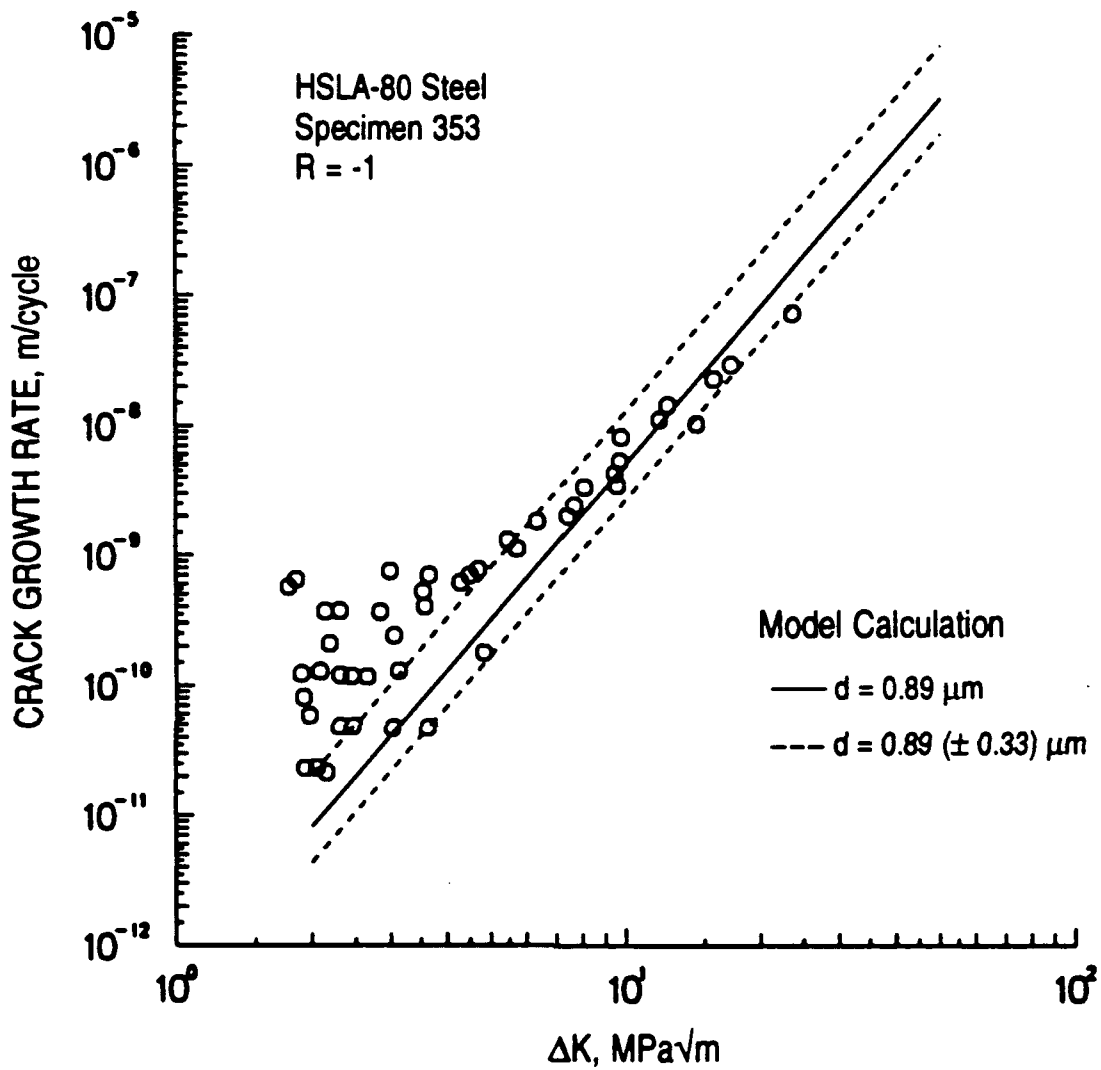


Figure 3. Comparison of small crack data with model calculations based on the average value and standard deviations of the mean-free-path of the Cu precipitates.

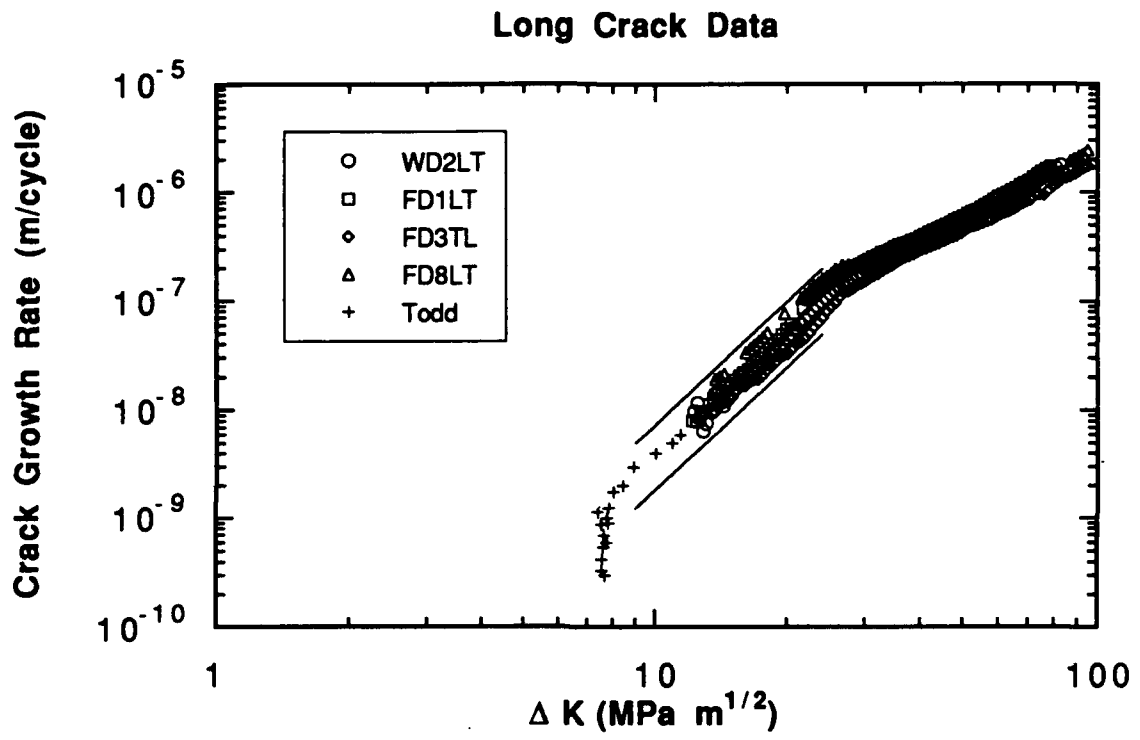


Figure 4. Large crack FCG data for HSLA-80 steel.

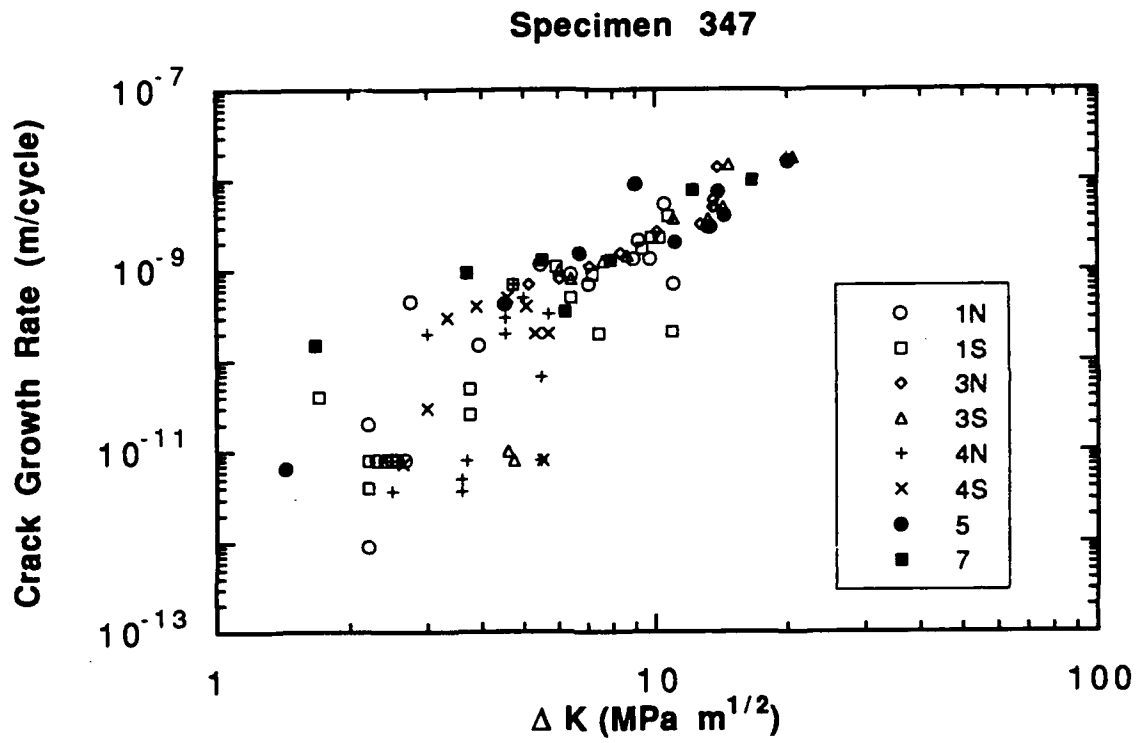


Figure 5. Microcrack FCG data from square beam specimen #347.

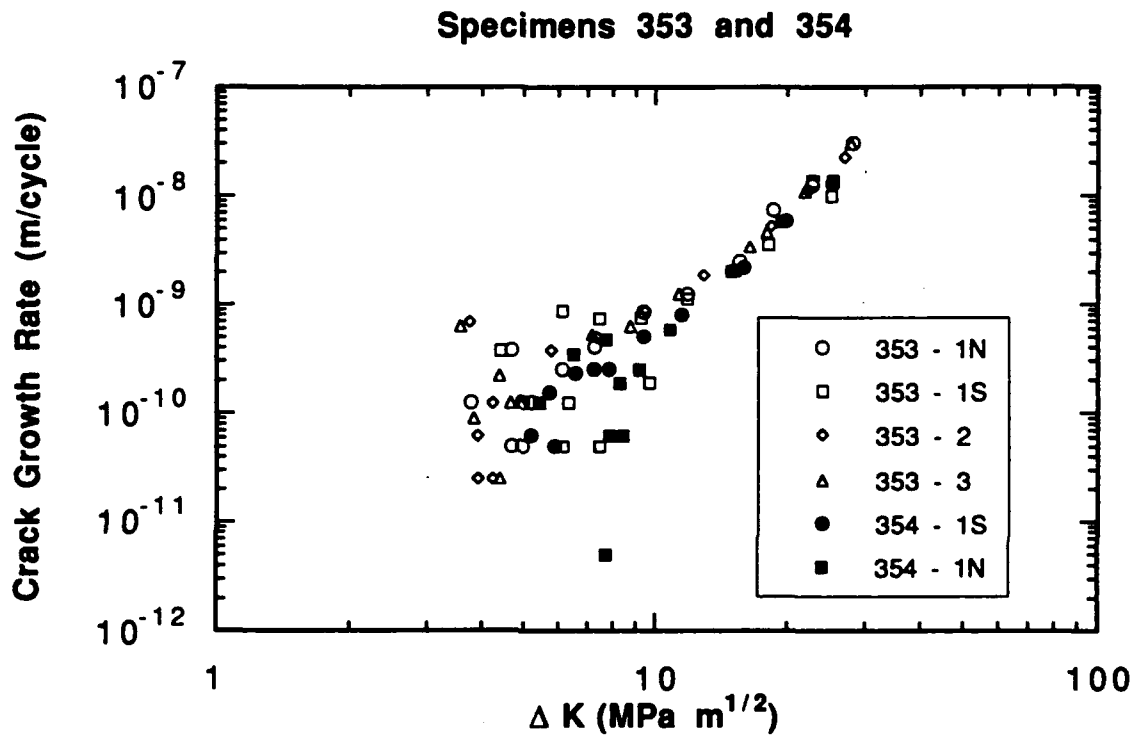


Figure 6. Microcrack FCG data from rotating beam specimens #353 and #354.

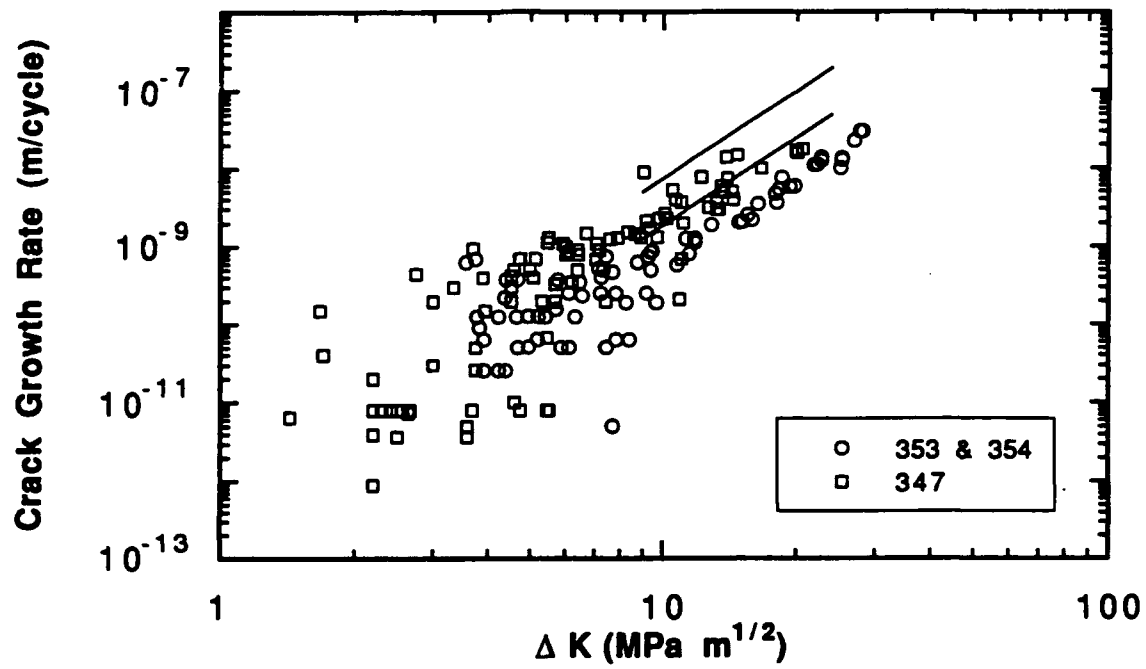


Figure 7. Comparison of large crack and microcrack data based on full range  $\Delta K$ .

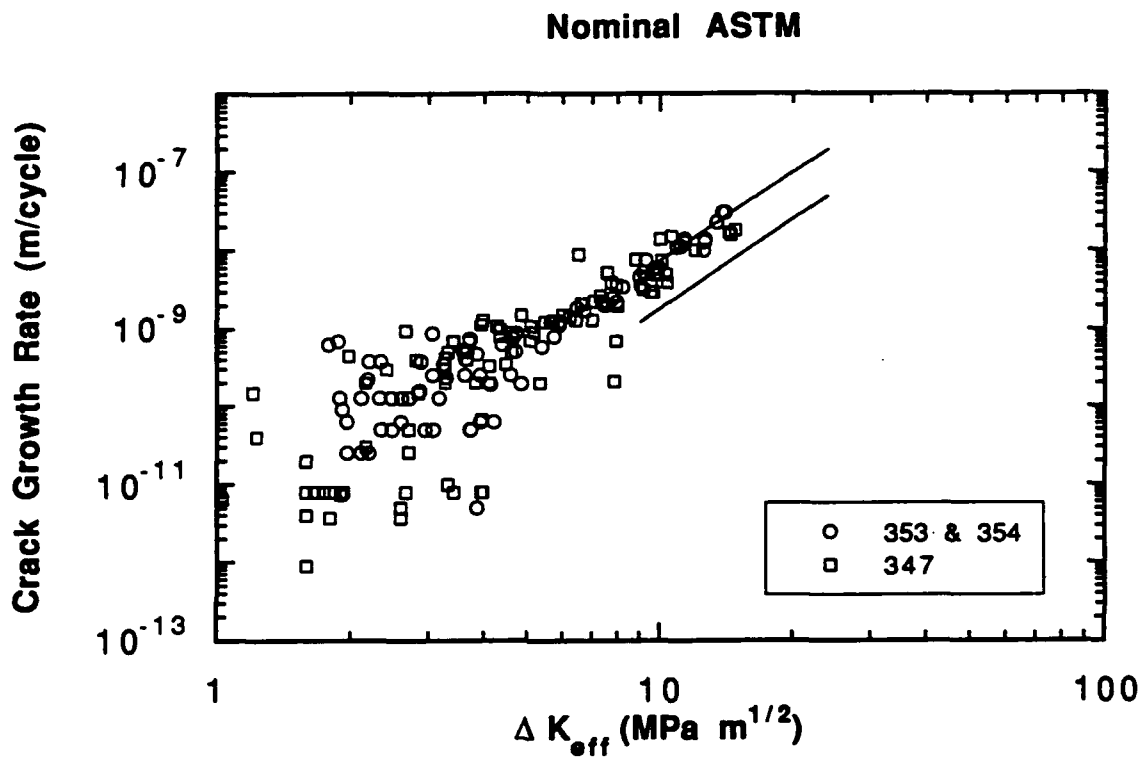


Figure 8. Comparison of large crack and microcrack data based on effective  $\Delta K$  defined by the nominal ASTM approach.

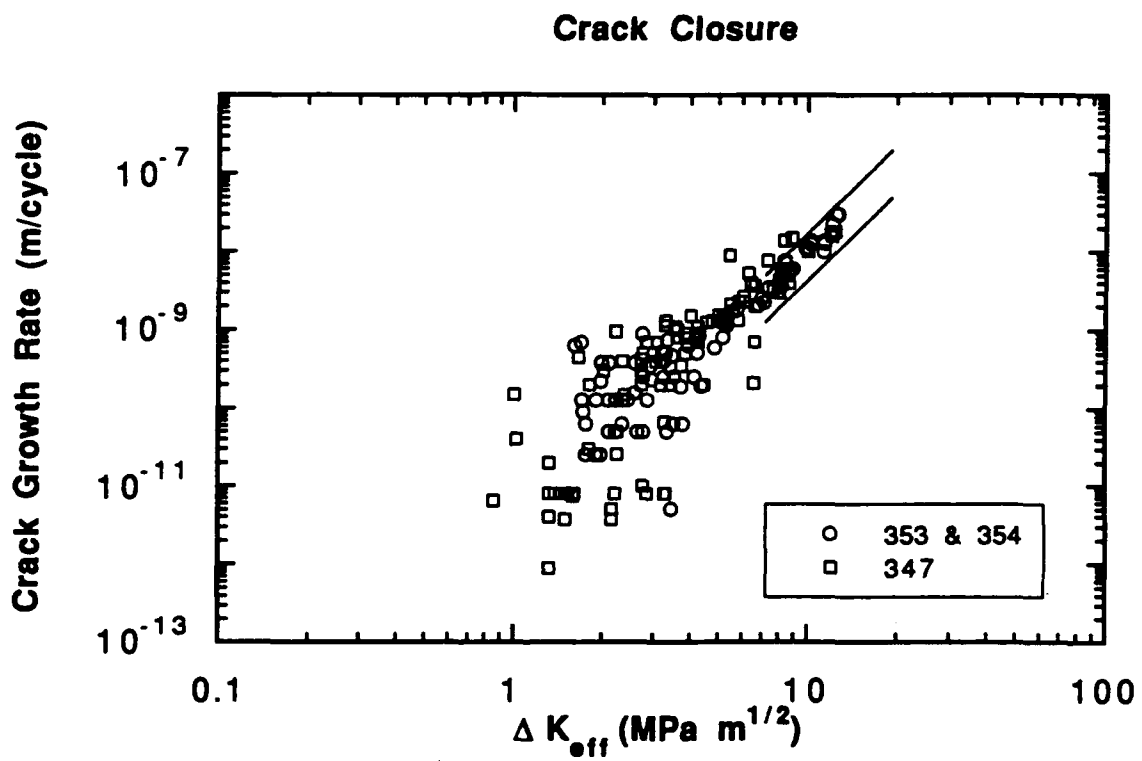


Figure 9. Comparison of large crack and microcrack data based on effective  $\Delta K$  defined by the Newman crack closure approach.

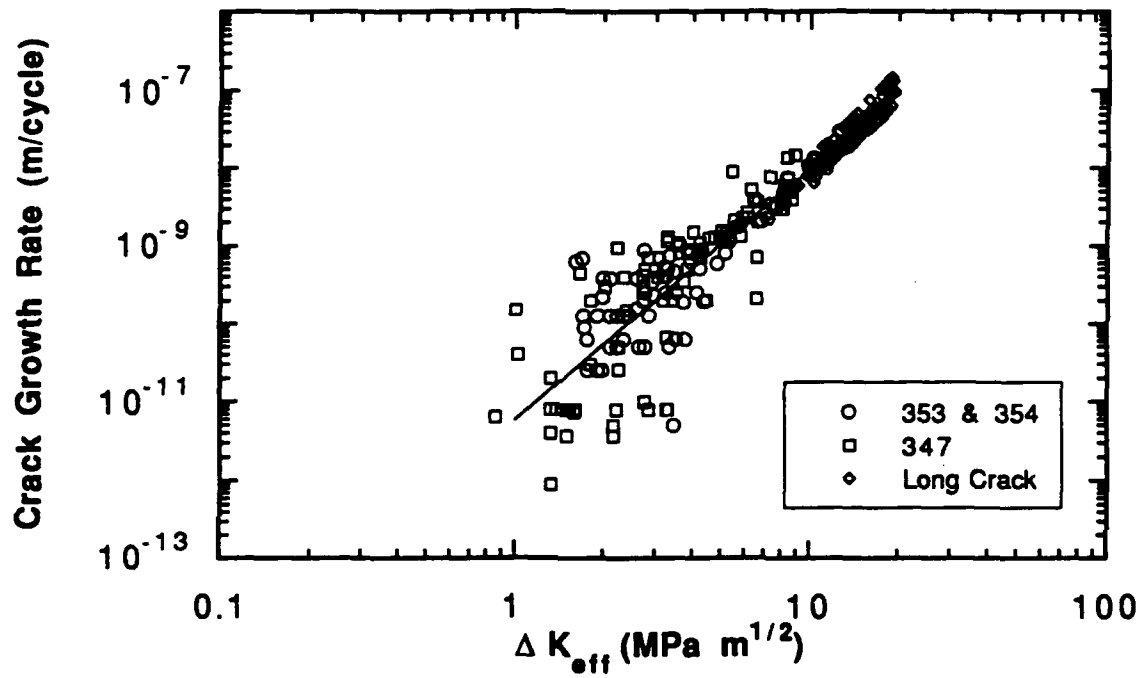


Figure 10. Comparison of large crack and microcrack data, showing linear regression of all combined data.

FATIGUE RESULTS OF ASTM A710 GRADE A PLATE AND WELDMENTS

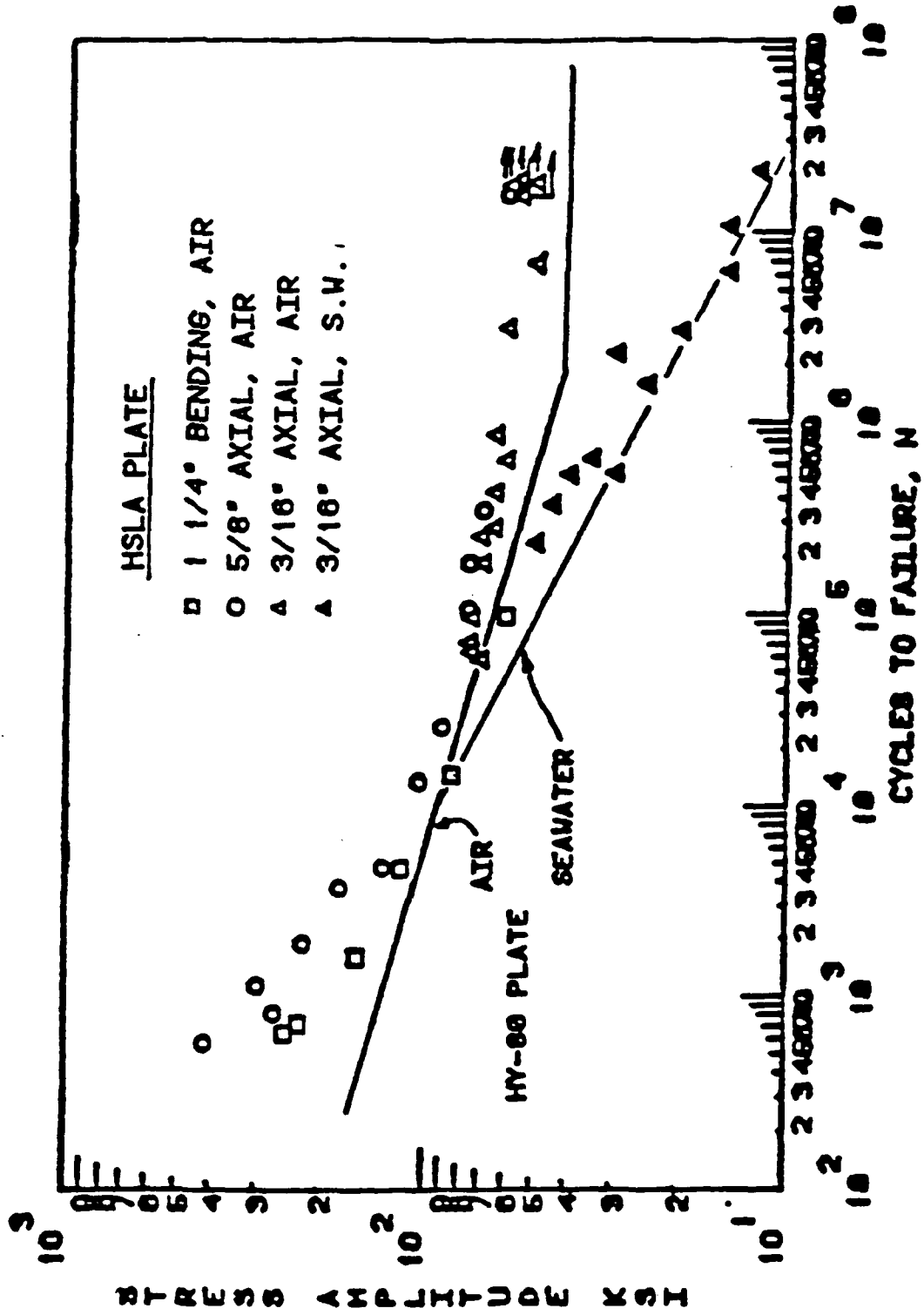


Figure 11. Smooth specimen S-N data for HSLA-80 [8].

# Simulated Bulkhead Attachments

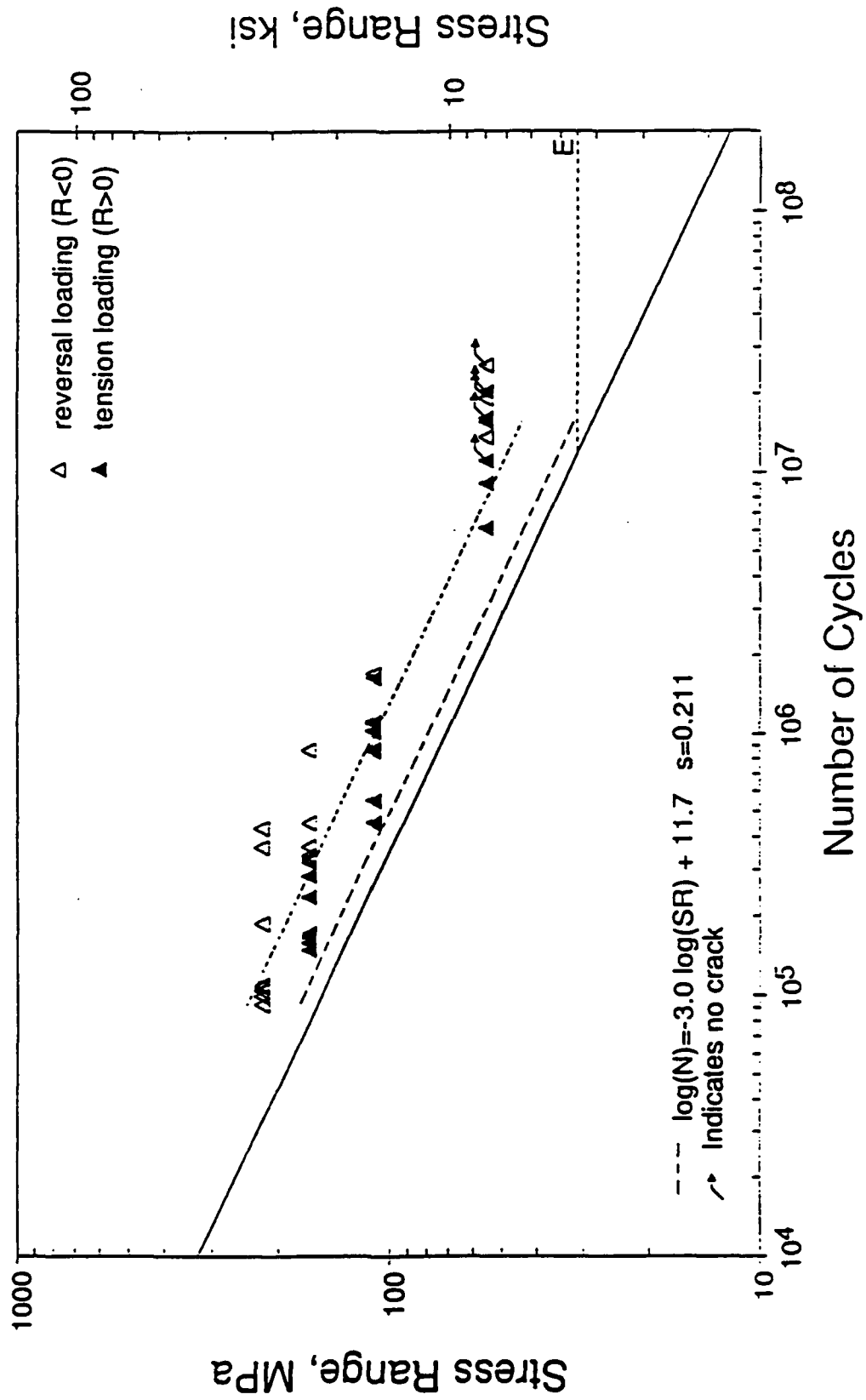


Figure 12. Welded structure S-N data for HSLA-80 [9].

# LOG(DK) VS. LOG(DADN)

#347 Data

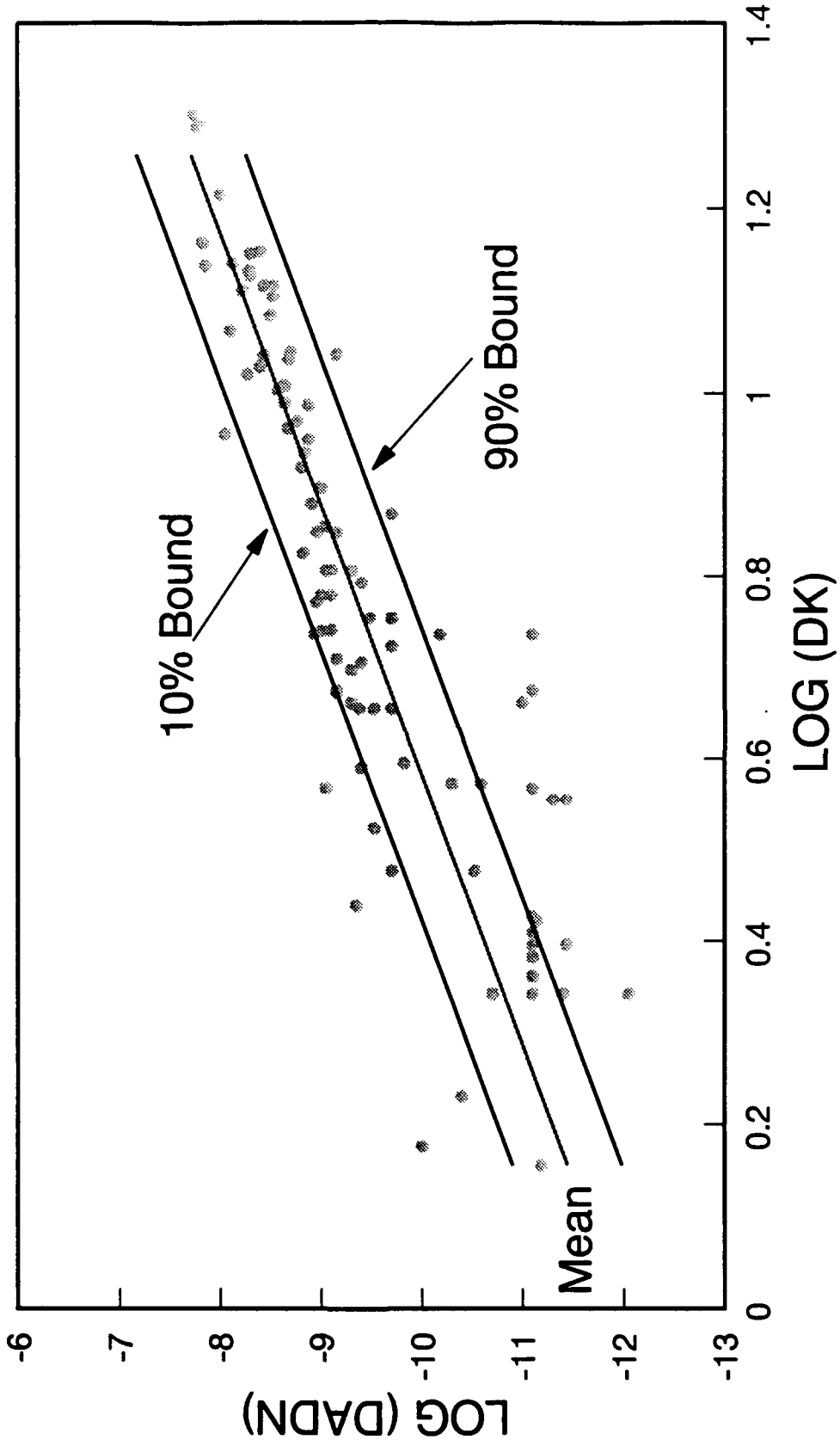


Figure 13. Illustration of the stochastic FCG model with data from specimen #347.

# LOG(DK) VS. LOG(DADN)

#353 and #354 Data

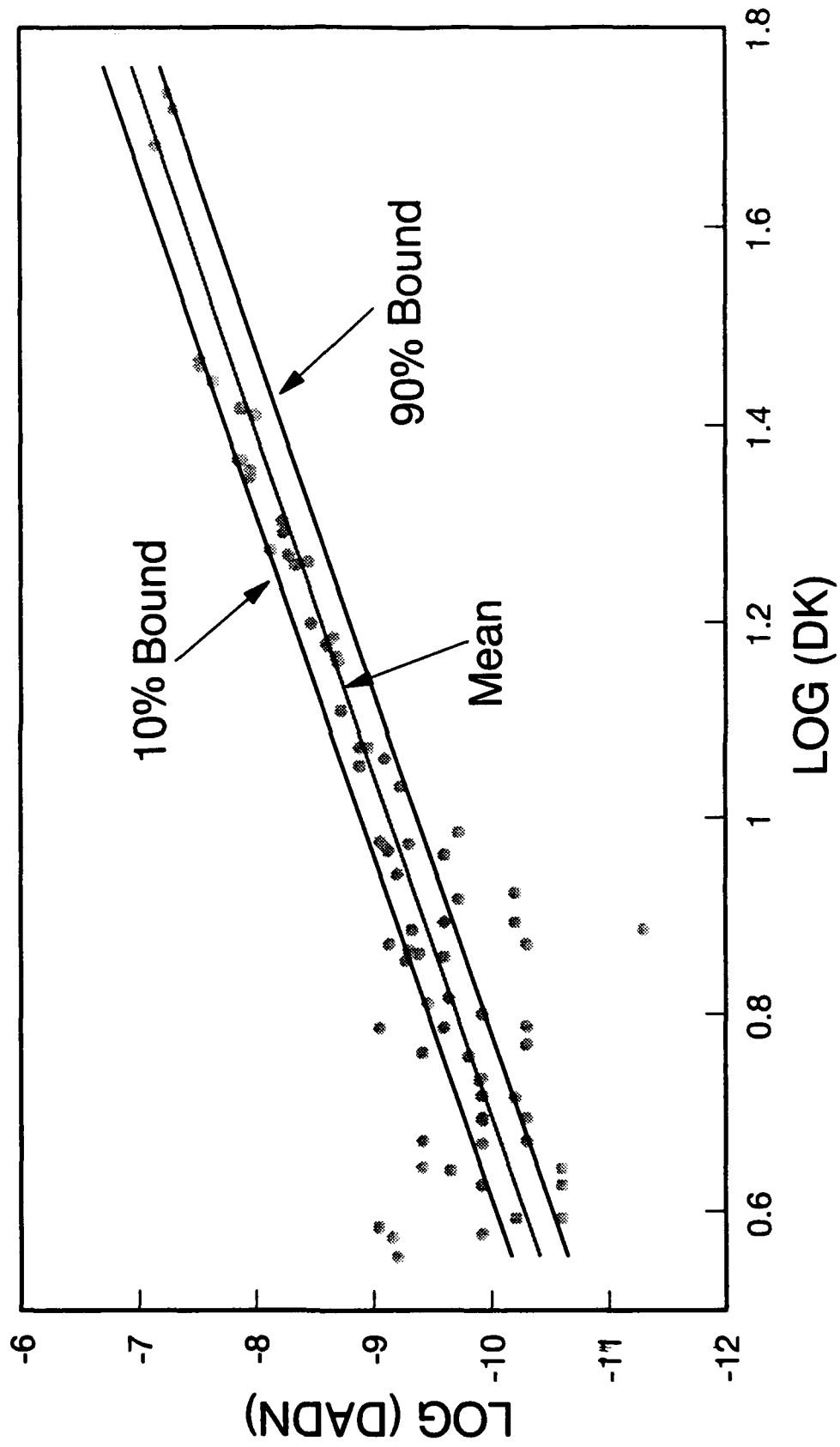


Figure 14. Illustration of the stochastic FCG model with data from specimens #353/354.

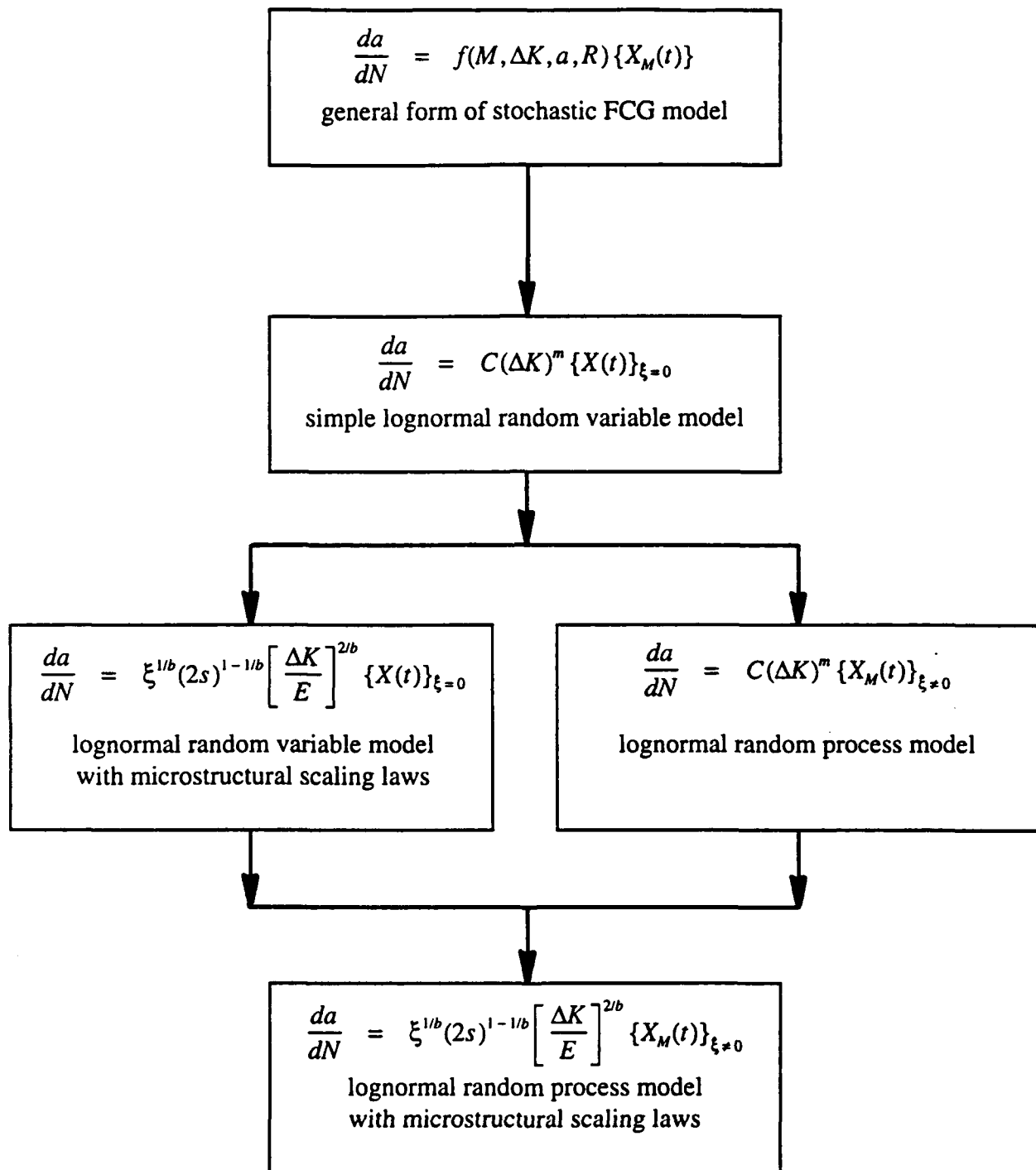


Figure 15. Overview of planned stochastic FCG model development.

# Crack Length vs. Cycle

#353 & #354

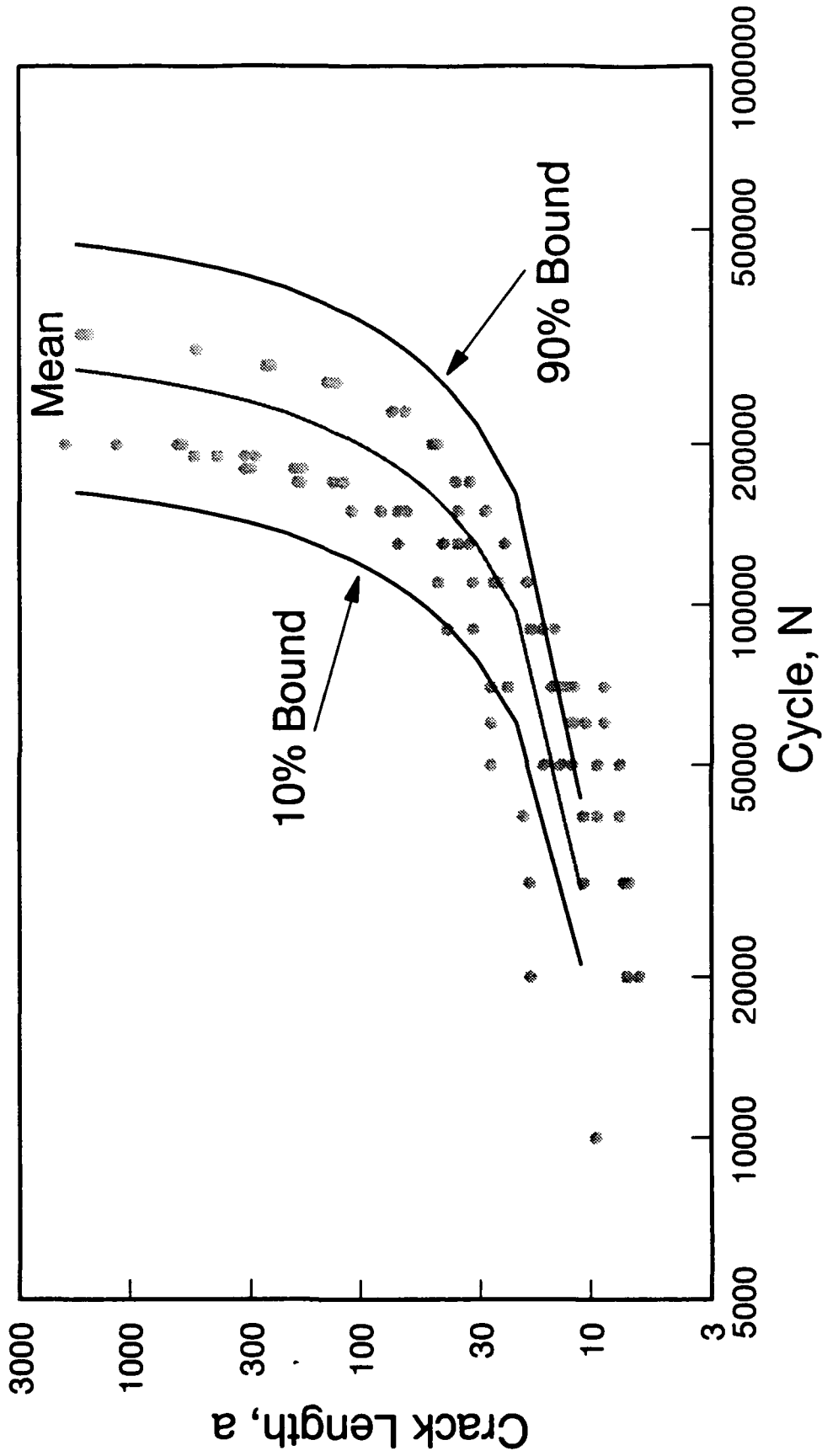


Figure 16. Fatigue life prediction for specimens #353/354.